Rev Environ Sci Biotechnol (2023) 22:397–426
https://doi.org/10.1007/s11157-023-09648-1

REVIEW PAPER

Cutting-edge technological advancements in biomass-derived hydrogen production

Shouvik Saha · Amita Mondal · Mayur B. Kurade · Yongtae Ahn · Priyabrata Banerjee · Hyun-Kyung Park · Ashok Pandey · Tae Hyun Kim · Byong-Hun Jeon

Received: 23 November 2022 / Accepted: 9 February 2023 / Published online: 24 February 2023

Abstract Production of hydrogen as carbon-free energy from renewable organic waste biomasses has been adopted for the long-term sustainability of a circular economy through various chemical and biological conversion processes. Conversion of waste biomasses to hydrogen provides dual benefits of low-cost energy-dense biofuel production and simultaneous waste reduction in eco-friendly valorization. Advancements in existing chemical and biological processes through light-induced photoreformation and microbial syntrophy-mediated metabolic induction in fermentation, respectively, facilitated holistic conversion of biowaste for maximum recovery of hydrogen by minimizing by-product generation. This review focuses on various thermochemical, photocatalytic reformation, and biological processes involving direct or indirect conversion of solid organic biomasses to hydrogen and their possible technological advancements to generate waste-to-value-added products. The techno-economic assessment describes the feasibility of waste biomass-derived hydrogen production over other technologies for industrial implementation.

S. Saha · A. Mondal · M. B. Kurade · Y. Ahn · B.-H. Jeon (✉)
Department of Earth Resources and Environmental Engineering, Hanyang University, Seoul 04763, Republic of Korea
e-mail: bhjeon@hanyang.ac.kr

A. Mondal · P. Banerjee
Surface Engineering and Tribology Group, CSIR-Central Mechanical Engineering Research Institute, Durgapur, West Bengal 713209, India

H.-K. Park
Department of Pediatrics, College of Medicine, Hanyang University, Seoul 04763, Republic of Korea

A. Pandey
Centre for Innovation and Translational Research, CSIR-Indian Institute for Toxicology Research, Lucknow 226001, India

A. Pandey
Sustainability Cluster, School of Engineering, University of Petroleum and Energy Studies, Dehradun 248007, India

A. Pandey
Centre for Energy and Environmental Sustainability, Lucknow 226029, India

T. H. Kim
Department of Materials Science and Chemical Engineering, Hanyang University, Ansan, Gyeonggi-do 15588, Republic of Korea

Graphical abstract

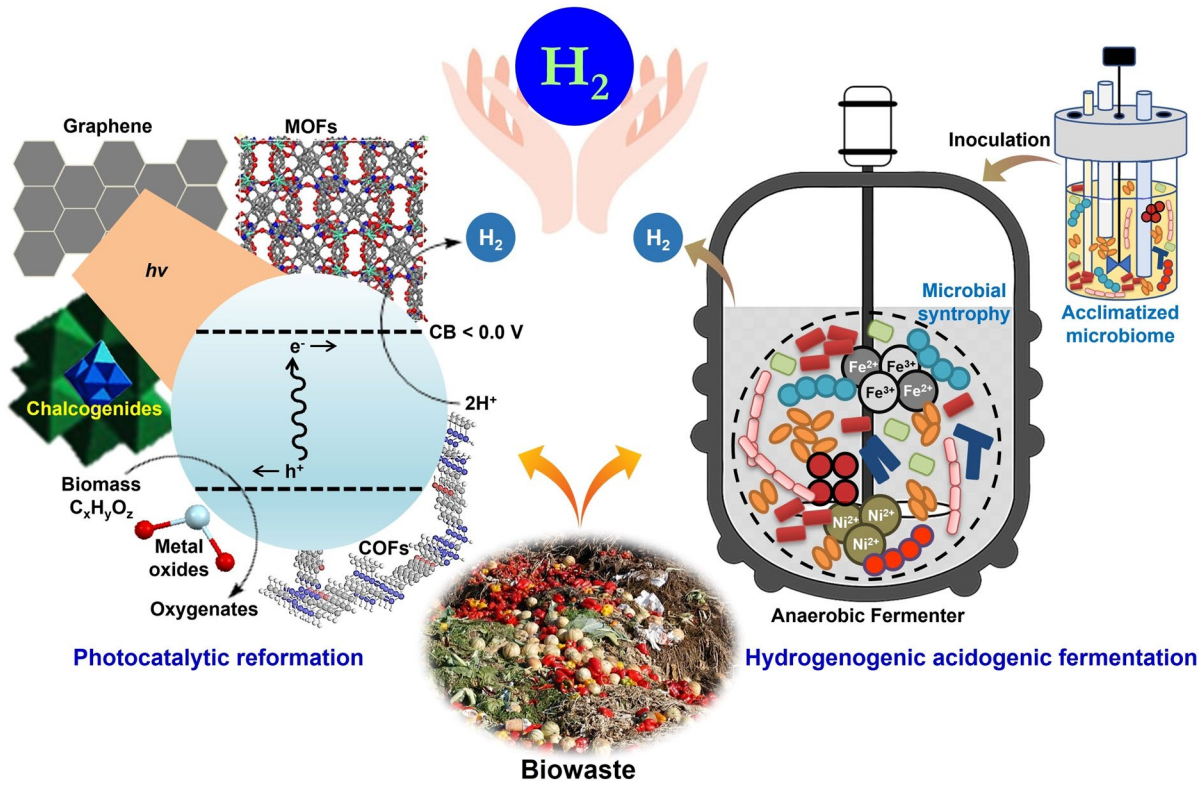

Keywords Hydrogen · Organic waste biomass · Gasification · Photocatalytic reformation · Hydrogenogenic acidogenic fermentation · Waste-to-value-added products

1 Introduction

Energy is a key part of sustainable societal advancement in the twenty-first century (Zhu et al. 2020). The worldwide energy consumption is expected to increase by 1.5% per year from ~ 1.8×10^5 terawatts (TW) in 2020 to approximately 2.6×10^5 TW by 2050 (Nalley and LaRose 2021). Intensive utilization of fossil fuel resources in industrial, municipal, and agricultural purposes continues to emit greenhouse gases, producing global warming and other negative consequences (Bajracharya et al. 2016). An ever-increasing worldwide demand for energy and the concomitant environmental pollution have led to the search for clean and sustainable energy systems (Saha et al. 2016). Renewable energy sources (e.g., wind, solar, and hydraulic power) are explored as feasible substitutions to conventional fossil fuels; however, their application is restricted due to spatial and temporal barriers (Zhu et al. 2020). Despite the increase in renewable energy usage, fossil energy resources remain a leading source of energy production, generating ~ 80% of overall energy (Tekade et al. 2020; Yuksel and Ozturk 2017). The CO_2 emissions are mainly produced from burning of fossil fuels, which also generates several other noxious gases, such as NOx and SOx. Such environmental issues motivated the scientific community in constant search for new alternative sources of energy, specifically renewable ones to reduce dependency on fossil fuels (Gao et al. 2018).

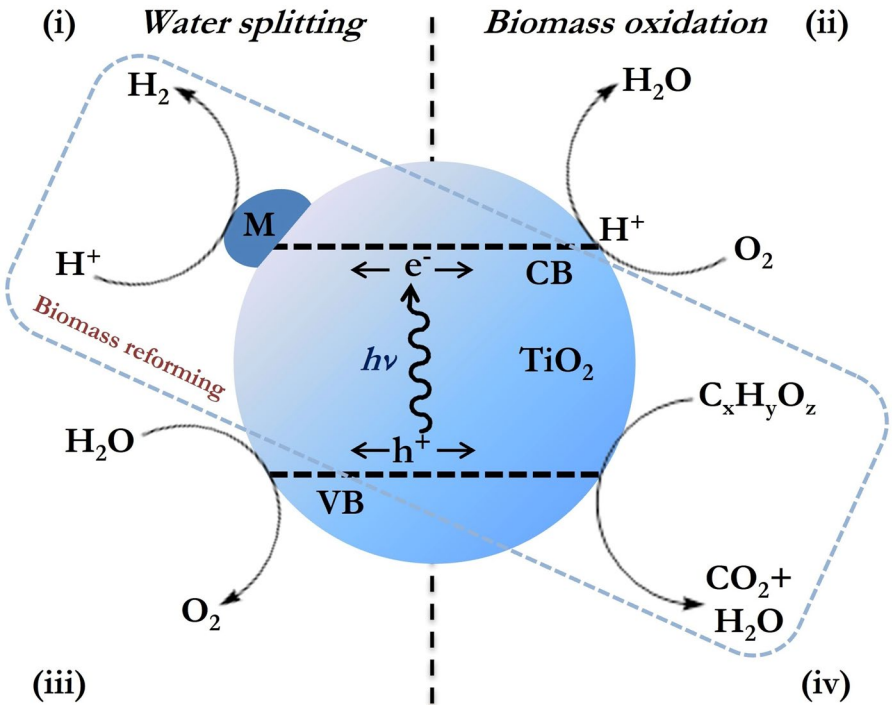

Fig. 1 Generation of H_2 (i) and O_2 (iii) through water splitting under anaerobic conditions. Oxidation of organic biomass-derived oxygenates (iv) occurs in aerobic conditions, followed by reduction to water (ii). All reactions require light absorption onto irradiated M/TiO_2 (M = noble metal) photocatalyst to generate separate charges, *i.e.*, e^- in the conduction band (CB) and h^+ in the valence band (VB). Thus, biomass photoreformation can occur under anaerobic conditions in combination with water splitting and biomass oxidation

Hydrogen (H_2), a carbon-free energy carrier with the highest known energy density (142 kJ g^{-1}), is considered a cutting-edge source of clean energy (Chang et al. 2018). Producing hydrogen through adaptable and eco-friendly processes is important for the sustainable hydrogen economy and future of clean energy (Tu et al. 2017; Zhu et al. 2020). However, conventional H_2 production from nonrenewable resources, *i.e.*, coal gasification, hydrocarbon reforming, plasma reforming, steam reforming of natural gas, water electrolysis, etc., is unsustainable for the circular economy due to their high carbon-footprint (~ 830 million tons per year) and energy-intensive process (Megía et al. 2021; Singh et al. 2015). Photocatalytic or photoelectrocatalytic green hydrogen production has gained attention for its long-term sustainability because it facilitates water splitting under visible light for solar-to-chemical energy; however, it provides low productivity of 5% (Hendi et al. 2020; Lu et al. 2017). Nonetheless, photocatalytic reforming or photoreforming through the combination of light-induced H_2 generation from water and oxygenated organic biomasses such as alcohols and carboxylic acids produced from biomass fermentation; saccharides; biopolymers has appeared to be a highly important intermediary route between photocatalytic water splitting and photo-oxidation (Fig. 1). The conversion of organic biomass-derived oxygenates into H_2 gas through photoreforming involves energy input in the form of light radiation (Puga 2016).

Utilization of renewable resources including organic waste biomasses (e.g., lignocellulosic agricultural wastes, fruit and food wastes, fat, oil and grease) and municipal/industrial wastewater for the production of H_2 appears to be the most convenient alternative to conventional processes for the reduction of production cost (Chang et al. 2018; Godvin Sharmila et al. 2022; Saha et al. 2019). Nearly 181.5 billion tons of lignocellulosic agricultural biomass is generated around the globe annually, although only a small percentage of it is refined and reused, leaving enormous amounts of organic waste (40–50% of their original mass) in the environment (Granone et al. 2018; Orozco et al. 2014; Talavera-Caro et al. 2020). The Food and Agricultural Organization of the United Nations estimated that the disposal of food waste has reached ~ 1.3 billion tons globally (Karmee 2016). Utilization of renewable wastes in hydrogen production diminishes their natural uncontrolled degradation and reduces the environmental threat of global warming (Saha et al. 2018). Adopting suitable approaches compatible with the circular economy concept to recycle renewable waste

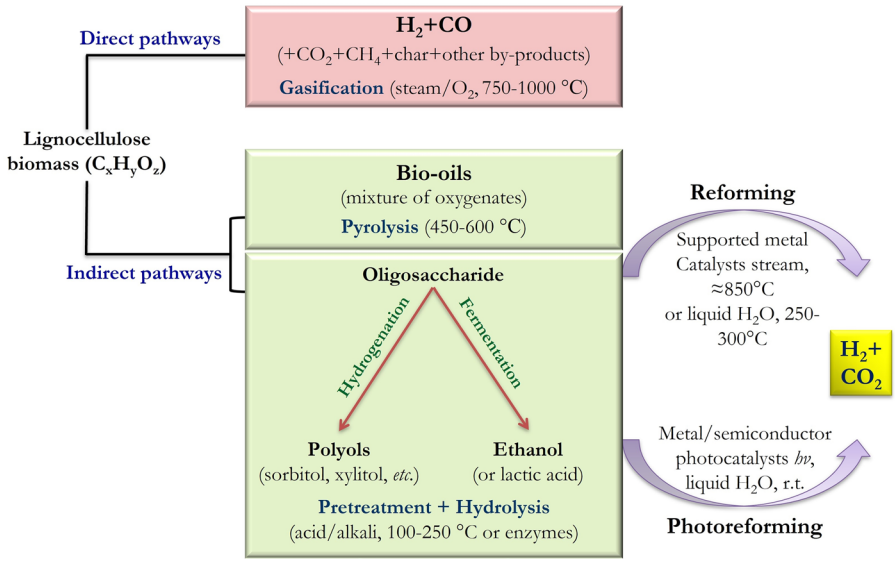

Fig. 2 Conversion of lignocellulosic biomass to produce H_2 through direct and indirect pathways

resources to generate hydrogen energy are necessary to limit uncontrolled degradation of these waste materials and their by-products (Kim et al. 2016). Small-scale, inexpensive, electron-driven chemical processes are crucial for decentralized transformation of biomass to produce high-value specialty chemicals or lower-value commodity chemicals or fuels (Akhade et al. 2020). Electrolytic hydrogen yields of $0.1-0.2$ mg mg^{-1} of raw biomass have been achieved at a cathode utilizing cellulose, starch, lignin, protein, and lipids of different biomasses (Hibino et al. 2018). Hydrothermal carbonization of food waste followed by steam gasification generated 28.08 mmol H_2 g^{-1} dry waste (Duman et al. 2018). The theoretical potential of hydrogen yield through hydrogenogenic dark fermentation of various lignocellulosic biomasses could reach 14–21 g H_2 kg^{-1} substrate (Sołowski et al. 2020). Therefore, waste organic biomasses could be an alternative feedstock for sustainable energy sources such as H_2.

In this relevance, this review discusses the fundamental and practical features of various biomass-derived hydrogen production technologies, including thermochemical, photocatalytic, and biological processes and their possible technological advancements to generate waste-to-value-added products. The assessment of techno-economic features describes the feasibility of biomass-derived hydrogen production for industrial implementation of advanced technologies.

Table 1 Reaction mechanisms and enthalpy of cellulosic biomass gasification reactions

Classification	Stoichiometry	Enthalpy (kJ g^{-1} mol^{-1}) at 300 K
Steam gasification	$C_6H_{10}O_5 + H_2O \rightarrow 6CO + 6H_2$	310
	$C_6H_{10}O_5 + 3H_2O \rightarrow 4CO + 2CO_2 + 8H_2$	230
	$C_6H_{10}O_5 + 7H_2O \rightarrow 6CO_2 + 12H_2$	64
Pyrolysis	$C_6H_{10}O_5 \rightarrow 5CO + 5H_2 + C$	180
	$C_6H_{10}O_5 \rightarrow 5CO + CH_4 + 3H_2$	300
	$C_6H_{10}O_5 \rightarrow 3CO + CO_2 + 2CH_4 + H_2$	− 142
Partial oxidation	$C_6H_{10}O_5 + 1/2O_2 \rightarrow 6CO + 5H_2$	71
	$C_6H_{10}O_5 + O_2 \rightarrow 5CO + CO_2 + 5H_2$	− 213
	$C_6H_{10}O_5 + 2O_2 \rightarrow 3CO + 3CO_2 + 5H_2$	− 778
Water–gas shift methanation	$CO + H_2O \rightarrow CO_2 + H_2$	− 41
	$CO + 3H_2 \rightarrow CH_4 + H_2O$	− 206

2 Hydrogen generation through chemical pathways

Production of hydrogen is feasible from biomass feedstock by numerous chemical and biological processes, including (1) direct gasification, where raw lignocellulose biomass is converted to syngas containing H_2 and CO as major constituents and (2) indirect conversion of biomasses to chemical intermediates and subsequent reformation, where oligomeric oxygenated compounds are formed by pyrolysis/hydrolysis followed by reformation into gaseous H_2 and CO_2 (Fig. 2) (Alonso et al. 2010; Navarro et al. 2009).

Biomass gasification is one of the oldest technologies to produce electricity and heat, having been employed since the 1940s (Huber et al. 2006a). In this process, liquid or solid carbonaceous substrates, such as lignocellulosic biomasses react with oxygen, air, and/or steam at comparatively lower temperatures (700–1000 °C) than coal gasification to form syngas, which consists of H_2, CH_4, CO, CO_2, and N_2. Combined reactions of steam gasification, pyrolysis, and partial oxidation result in solid, liquid, and gas phases in biomass gasification (Table 1) (Puga 2016). In steam reforming, the feedstock is reacted with water to yield CO_2, CO, and H_2. Pyrolysis involves thermal disintegration of the biomass feedstock into solid, liquid, and gaseous products in absence of steam or oxygen. Partial oxidation methods involve less O_2 than required by stoichiometry for combustion. The water–gas shift reaction (WGSR, where generation of H_2 and CO_2 occurs through a reaction between CO and water) and water–gas shift methanation (where the interaction of H_2 and CO produces H_2O and CH_4)

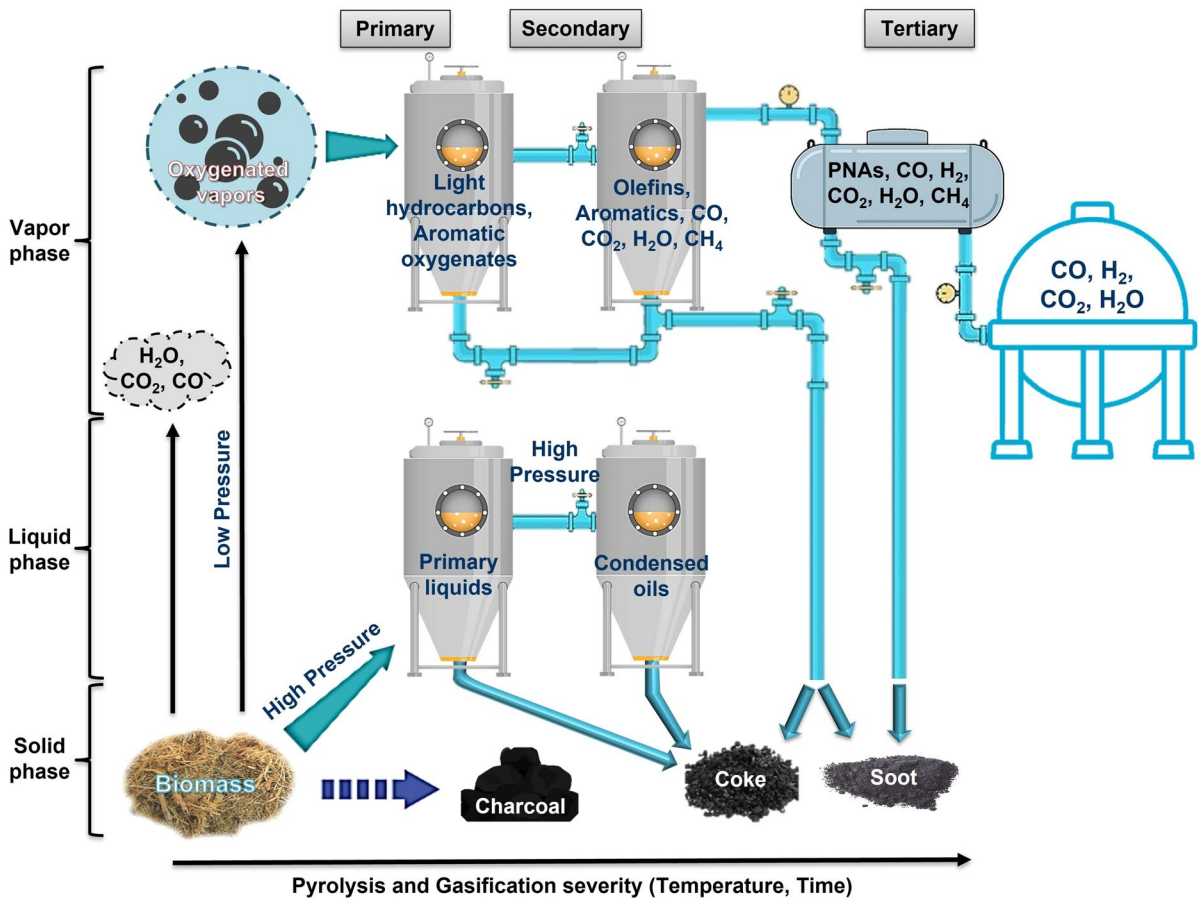

Fig. 3 Process elucidating the biomass gasification. Pyrolysis and gasification severity increase with temperature and time in direct gasification of biomass, producing H_2, CO_2, CO, and H_2O as major products

also take place in gasification. To promote the gasification reactions, heat is produced through direct gasification (exothermic reaction and partial combustion within the gasifier generate heat) or indirect gasification (heat is formed at the outer part of the gasifier and moves inside) (Sikarwar et al. 2016).

2.1 Direct gasification

The direct gasification method involves primary, secondary, and tertiary processes (Fig. 3). In the first gasification stage, gaseous CO_2, H_2O, oxygenated vapors, and primarily oxygenated liquids are produced as main products from solid biomass along with a few by-products including cellulosic molecules, lignin-based methoxyphenols, hydroxyacetaldehyde, levoglucosan, and their corresponding hemicellulosic derivatives (Usino et al. 2021). Initial pyrolysis of the organic substances generates nonreactive lower-molecular weight vapor containing monomers and their fragments. This vapor is free of cracking derivatives of subsequent gas-phase reactions. Charcoal is produced from slow pyrolysis, which preserves the characteristics of lignocellulose. In the second step, the primary liquids and vapors produce gaseous aromatics, olefins, CO_2, CO, H_2, H_2O, and secondary compressed oils like aromatics and phenols. The primary vapors create cracking (regimes of secondary interaction) in the biomass upon heating above 500 °C, while the temperature regime of the secondary reaction is within 700–850 °C. The products from the secondary reaction enter the tertiary reaction as temperature increases to 850–1000 °C, generating CO_2, CO, H_2O, H_2, and polynuclear aromatics (PNA) substances containing methyl-derived aromatics like methyl naphthalene, methyl acenaphthylene, indene, and toluene (Sikarwar et al. 2016). A liquefied tertiary phase is generated from condensation of some tertiary substances including naphthalene, benzene, anthracene/phenanthrene, acenaphthylene, and pyrene. Coke and soot are generated during the secondary and tertiary reactions. Coke is produced through thermolysis of organic vapors and liquids, while the decomposed yields of hydrocarbons after homogeneous nucleation at high temperature in the gaseous state produce soot (Alonso et al. 2010). Usually, the inorganic constituent of the gasification feedstock is transformed into bottom ash (further eliminated from reactor) or fly ash (leaves along with product gas). The constituents of ash include K_2O, CaO, P_2O_5, SiO_2, MgO, Na_2O, and SO_3. The operating temperature should be below 1000 °C (at which ash melts) to restrict slagging and sintering of ash (Herman et al. 2016).

The composition of gas released from the gasification vessel is dependent upon the composition of biomass feedstock, the gasifying mediator, and the gasification method (Navarro et al. 2009). Tars containing heavier hydrocarbons cause clogging and blocked filters as they agglomerate on certain filters and in downstream pipes (Devi et al. 2003). Tars can also produce other downstream complications and choke fuel outlines and injectors in interior combustion engines. Choosing a suitable gasification reactor and conditions can reduce the quantity of tars. Addition of solid catalysts including Ni, Pd, Pt, and Ru, reinforced on dolomite, $Rh/SiO_2/CeO_2$ and CeO_2/SiO_2 within the gasification vessel can reduce the concentration of tar (Tomishige et al. 2004). Wet impregnation or dry mixing of alkali metal catalysts including K_2CO_3, $Na_3H(CO_3)_2$, Na_2CO_3, $CsCO_3$, $Na_2B_4O_7{\cdot}10H_2O$, NaCl, $ZnCl_2$, KCl, and $AlCl_3{\cdot}6H_2O$ with biomass derivatives can decrease tar generation (Sutton et al. 2001). However, alkali metals are not profitable due to char formation, increased ash content, reduced carbon transformation, and the complicated recycling process. Nevertheless, a mixture of CO, H_2, CO_2, and some CH_4 is produced along with other gaseous ingredients and solid offshoots like char through a one-step transformation of raw or mechanically pretreated biomass feedstock in a direct gasification process under oxygen and steam environments at high temperature (750–1000 °C) (Alonso et al. 2010; Navarro et al. 2007). Tar generation can be reduced through movement of the gaseous products of the secondary reaction over the char bed as a catalyst (Sikarwar et al. 2016). Despite its limitations of harsh conditions, this adaptable gasification process can be altered for a varied array of biomass derivatives to achieve hydrogen yields of 50–80 g H_2 kg^{-1} biomass (Parthasarathy and Narayanan 2014).

2.2 Indirect processes based on reforming and photoreforming of oxygenates

2.2.1 Reforming of oxygenates

The indirect process is a combination of primary liquification by pyrolysis to produce bio-oils and mixed oxygenated elements and by pretreatment/hydrolysis and fermentation of cross-linked, heavier biopolymers (lignin, hemicellulose, and cellulose) into mixed oxygenated chemical ingredients having lower molecular weight, followed by catalytic reformation (Demirbaş 2001; Zinoviev et al. 2010). Producing H_2 via reformation of pyrolysis oils is a consistent route for reclamation of complex and unstable biomasses such as lignocellulosic agricultural wastes, food waste, biopolymers, etc. H_2-enriched gaseous streams are produced by reforming bio-oils in water (either liquid or steam) at high temperatures (~ 850 °C) with low retention time on reinforced Ni or noble metal catalysts (Rioche et al. 2005). Another procedure involves reformation in aqueous phase under milder temperatures (250–350 °C) (Vispute and Huber 2009). Nevertheless, the required temperatures for the reforming processes are high (250–850 °C) in both cases. Compounds with functional groups like carboxylic acids or carbonyls can be degraded (through condensation, cyclisation, etc.), while saccharides can be decomposed by dehydration, polymerization, and so on. Therefore, thermo-catalytic reforming suffers due to formation of unwanted carbonaceous byproducts, which can deactivate the catalyst and initiate pyrolysis of saccharides even before their interactions with catalyst media to form CO in large amount (Fu et al. 2005).

Reforming of various oxygenates derived from hydrolysis of lignocellulose in an aqueous phase followed by sequential transformations is another indirect pathway for biomass-to-hydrogen production (Cortright et al. 2002; Huber et al. 2003). As stated by Dumesic et al., usage of appropriate catalysts such as Pd, Pt, or Ni–Sn catalysts (desirably sustained on Al_2O_3) can regulate the selectivity of this process by minimizing alkane production (Davda et al. 2005). These catalysts are highly active for water–gas shift reactions (WGSR), C–C scission, and dehydrogenation to produce fewer side reactions, such as methanation or C–O scission. The formation of light oxygenates from lignocellulosic biomass and its subsequent reformation in the aqueous phase to yield H_2 selectively at milder conditions in comparison to the one-step processes (gasification) indicates the indirect process as a candidate for biomass-to-hydrogen production. However, the thermo-catalytic aspect is energy exhaustive and might require high pressures (~ 35 bar) and temperatures (550–900 °C) (Lewis et al. 2003; Naikoo et al. 2021). This causes side reactions or degradation, which have unfavorable impacts on H_2 selectivity (50–60% of the theoretic maximum) and produce excessive amounts of alkanes (Huber and Dumesic 2006). In this scenario, methods of augmenting the reformation (Eq. 1) while limiting other conversions are desired and would be advantageous for biomass-derived H_2 production technologies.

$$C_xH_yO_z + (2x - z)H_2O \rightarrow (2x + y/2 - z)H_2 + xCO_2 \quad (1)$$

There are four substantial reformation technologies for transforming biomass to hydrogen: catalytic steam reforming (CSR), catalytic partial oxidation (CPO), auto-thermal reforming (ATR), and aqueous phase reforming (APR) (Zinoviev et al. 2010). CSR, the conventional reforming process, is adopted to produce H_2 from fossil hydrocarbons, specifically methane. This technique is used to treat oxygenated substrates ($C_nH_mO_k$, Eqs. 2 and 3) along with stoichiometric WGSR process for augmenting H_2 production.

$$C_nH_mO_k + (n - k)H_2O \leftrightarrow nCO + (n + m/2 - k)H_2 \quad (2)$$

$$C_nH_mO_k + (2n - k)H_2O \leftrightarrow nCO_2 + (2n + m/2 - k)H_2 \quad (3)$$

Reforming of biomass derivatives such as methanol, glycerol, ethylene glycol, and sorbitol is thermodynamically more promising at low temperatures (~ 277 °C) with respect to hydrocarbons having similar numbers of C atoms (Davda et al. 2005). Therefore, the reforming procedure is more suitable for use with the WGSR than is hydrocarbon reforming as there is a possibility of further reactions of CO_2 and CO with H_2 at lower temperatures (27–377 °C), producing alkanes by Fischer–Tropsch synthesis (FTS) or methanation (Shabaker et al. 2004; Vaidya and Lopez-Sanchez 2017). In addition, gas phase homogeneous thermal disintegration of oxygenated

hydrocarbons and cracking reactions (Eq. 4) on the acidic parts of the catalytic surface decrease the selectivity and disable the catalyst.

$$\begin{aligned} &C_nH_mO_k \rightarrow C_xH_yO_z \\ &+ \left(H_2, CO, CO_2, CH_4, \text{Hydrocarbons}\right) + \text{coke} \end{aligned} \quad (4)$$

Coke formation over the catalyst support is facilitated during the reformation of oxygenated organic substances because of higher molecular weights, more instauration, and aromaticity. Hence, reforming requires specific biomass characteristics such as less molecular weight, saturation, and non-aromaticity to curtail the generation of or eliminate coke byproducts from the catalyst by steam gasification.

CPO (Eq. 5) is a noteworthy alternative to CSR technology, where the fuel interacts with a lower amount of oxidizer (O_2) than that required by stoichiometry for complete combustion.

$$C_nH_mO_k + (n - k/2)O_2 \rightarrow nCO_2 + \left(\frac{m}{2}\right)H_2 \quad (5)$$

The CPO process has several advantages over the CSR method, such as lack of coking, smaller reactor size, and facile CO_2 recovery. Nevertheless, this process has risks associated with explosions, specifically in the region of premixing, while maintaining the stability of the catalyst is also critical. The process has been well-explored for H_2 production from lightweight alcohols compared to complex oxygenated substances (Liguras et al. 2004; Miyazawa et al. 2006; Navarro et al. 2007). The autothermal reforming (ATR) process is a combined CPO and CSR approach providing a thermally self-sustaining faster method, where oxygen, hydrocarbons/oxygenated hydrocarbons, and steam are reactants (Eq. 6).

$$\begin{aligned} &2C_nH_mO_k + (2n - k/2)H_2O + (n - k/2)O_2 \rightarrow \\ &2nCO_2 + (2n + m - k)H_2 \end{aligned} \quad (6)$$

In contrast, aqueous phase reforming (APR) is an adaptable single-step technology for biomass derivatives (oxygenated alcohols, sugars, glycerol, ethylene glycol) to produce H_2, using reinforced metals and metal amalgams in the form of heterogeneous catalysts (Chheda et al. 2007; Cortright et al. 2002). This process involves the breakage of C–C and C–H and/or O–H bonds to produce adsorbed species over the catalyst support. There are several advantages of the APR process in comparison to CSR, including (1) no need to vaporize the feed, (2) use of relatively high pressures (15–50 bar) and low temperatures (150–270 °C) that promote the WGSR and yield a small amount of CO (< 1000 ppm), (3) use of low temperatures to reduce unwanted disintegration reactions like cracking, and (4) use of high pressures to support the refinement of H_2 (*e.g.*, by membranes or PSA) by sequestering CO_2 (Ghasemzadeh et al. 2016; Huber et al. 2006b). However, use of expensive noble-metal-assisted catalysts at high pressure for an elevated reaction time increases the unit cost of H_2 production from dilute feedstock solutions in this process. The use of strong mineral acids in the aqueous phase leads to the leaching of the active noble metal in the solution, which limits the recyclability of the catalysts and causes corrosion in the reactor. Aqueous discharges of this process also pose serious environmental concerns due to the leaching of metal catalysts (Vaidya and Lopez-Sanchez 2017).

Separation of hydrogen from the mixture of gaseous contaminants requires separate purification/refinement processes. The selection of a suitable H_2 purification method is dependent on the concentrations and downstream impacts of contaminants like N_2 and CO (Santhanam et al. 2017). The biomass-derived H_2 contains several gaseous contaminants including O_2, CO_2, CO, CH_4, and moisture. The foremost H_2 refining technologies can be divided into four categories of (1) physical adsorption (Liu et al. 2009), (2) chemical absorption, (3) cryogenic processes (Lu et al. 2007), and (4) membranes (Bernardo et al. 2010, 2009; Drioli and Giorno 2009). In this context, WGSR plays pivotal role in regulation of the CO/H_2 levels as CO forms CO_2 and H_2 upon interaction with water (Table 1). Industrial H_2 generation by the WGSR is performed in a set of two reactors: (1) a high-temperature WGS reactor at 350–500 °C having a Fe-oxide-mediated catalyst and (2) a low-temperature WGS reactor at 200 °C possessing Cu-functionalized catalyst (Bartholomew and Farrauto 2010). In the first reactor, the concentration of CO decreases to ~ 2–3%, which reduces further to ~ 0.2% in the second reactor under low-temperature. Pressure swing sorption, preferential air oxidation (PROX), and Pd membranes can be used to produce highly purified H_2 (Rostrup-Nielsen 2001). Nanometer-sized Au-amended catalysts are highly effective for oxidation of CO in WGSR (Carrettin et al. 2004; Fu et al. 2005, 2003). Kim et al. developed an alternative

to the WGS called the PROX method, where CO is transformed to CO_2 and electrical energy at higher rates by consuming aqueous polyoxometalates (POM) in comparison to the WGSR (Kim et al. 2005a, 2004). The complete reaction involves oxidation of CO and H_2O to produce CO_2 and protons with POM, *e.g.*, $H_3PMo_{12}O_{40}$, in the presence of Au catalyst. The aqueous and reduced mixture of POMs and H^+ can be utilized to generate electricity at the anode of a proton exchange membrane (PEM) containing fuel cell (Kim et al. 2005b). In this method, the POM solution is re-oxidized, and the consumption rate of CO (as turnover frequency of 0.75–5 s^{-1}) is greater than that of WGS at room temperature.

2.2.2 *Photoreforming of oxygenates*

Light-driven oxygenate reformation to produce H_2 and CO_2 upon suitable photocatalytic substances has excellent potential to drive next generation advancements. This technique involves effective reformation of various oxygenates (that can be biomass derived) including alcohols, carboxylic acids, saccharides, polymers in an aqueous medium using semiconductor-supported photocatalysts. Operation at 20–60 °C during the reaction minimizes the scope of degradation and creates high H_2 selectivity (Chen et al. 2010). Kondarides and colleagues demonstrated transformation of typical biomass-based oxygenates such as alcohols, glycerol, saccharides, biopolymers to H_2 on Pt/TiO_2 photocatalysts simulated by sunlight without deactivation (Daskalaki and Kondarides 2009; Kondarides et al. 2008). In some cases, the reformation process is endergonic ($\Delta G^0 = 237$ kJ mol^{-1}), which signifies the storage of solar energy into the produced products as chemical energy and increases the total heat content of the produced fuel (Cargnello et al. 2011). The photocatalytic reformation of biomass oxygenates broadens the selection routes for direct H_2 generation because it involves inexpensive feedstocks and solar light as the energy source, and the process is proficient, adaptable, and energy efficient. Solid materials consisting of light-absorbing semiconductors such as Au/TiO_2, $Pt/Ti\text{-}MOF\text{-}NH_2$, $Ni/Au/TiO_2$ along with metallic co-catalysts act as photocatalysts during H_2 evolution from aqueous phase. The semiconductors allow formation of charge transporters (electrons and holes) through light absorption, and they transfer to the substance surfaces, where the redox reaction occurs. Therefore, the semiconductor band gap must be matched with the incident photon energy. That is, the electrons are promoted from their valence to conduction band at a shorter wavelength compared to the material absorption as dictated by its band gap. The electron transfers from the conduction band to acceptor, and donor to valence band–hole annihilation occurs only when the energy points are respectively higher and lower than the consistent redox pairs. Co-catalysts are usually integrated on the semiconductor surface and can improve the efficiency by delivering active parts for H_2 evolution by reducing protons or associated substances. At the oxidation half reactions, the semiconductor surface itself catalyzes the transfer of holes to oxygenates or electron from oxygenates to the semiconductor with associated extinction of the photogenerated holes (Fang and Shangguan 2019; Hu et al. 2014; Sun et al. 2019b).

Oxide semiconductors having d^0 or d^{10} metals are considered the most efficient photocatalysts. TiO_2 is generally the ideal semiconductor to design heterogeneous photo-catalysts and anodes (Martha et al. 2015; Naldoni et al. 2019). The conduction band energy is slightly higher than the redox potential of H^+/H_2 in TiO_2, and band flexibility imparts additional advantages in the H_2 formation reaction in solution (Fig. 4a). Light-triggered electrochemical water splitting can be achieved using platinum black as a cathode and rutile TiO_2 as the photoanode (Fujishima-Honda process). The high photoactivity of TiO_2 in oxidation half-reactions increased its popularity for light-stimulated H_2 production from various oxygenated biomass feedstocks (Schneider et al. 2014). Nevertheless, enhanced surface area with availability of more surface sites, superior crystallinity, and lesser propensity toward electron–hole rearrangement enhances the efficiency of TiO_2 (Moretti et al. 2014). Similarly, WO_3 amended with Pt/Au or SnO_2/self-doped with Sn (II)/co-doped with Ce and Sb can catalyze photoreformation of biomass-derived glycerol (Liu et al. 2015a; Tanaka et al. 2014). ZnO has also demonstrated noteworthy photoactivity to produce H_2 from methanol or formaldehyde (Guo et al. 2015). ZnO nanoroads formed on graphene showed high efficiency for glycerol photoreformation under Xe light, while generation of ZnS in the presence of thiosulfate anions mediated hydrothermal treatment and improved the efficiency (Bao et al. 2015; Lv et al. 2015). NiO, ZnO, CuO, Cu_2O, Fe_2O_3, Co_3O_4, and

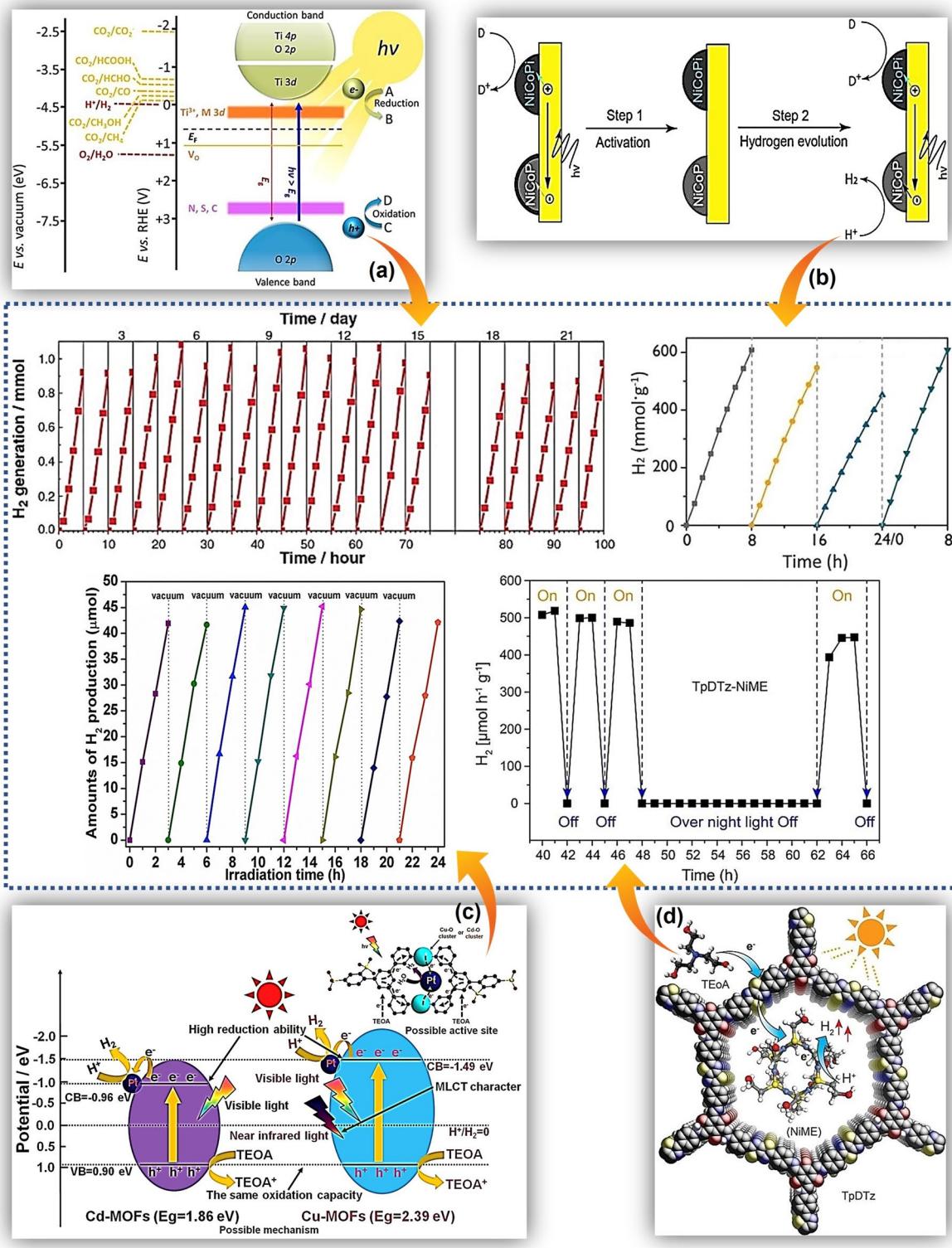

Fig. 4 Generation of H_2 through photoreformation using semiconducting photocatalysts of TiO_2 (**a**), CdS (**b**), Cd-MOF and Cu-MOF (**c**), and TpDTz COF (**d**) (Biswal et al. 2019; Naldoni et al. 2019; Song et al. 2017; Zhao et al. 2020)

VO_2 also showed high efficiency in the photoreformation process. Mixed oxides including $SrTiO_3$ (Peng et al. 2015a), $BiVO_4$ (Xue and Wang 2015), and Bi_2WO_6 (Panmand et al. 2015) have recently emerged as excellent photocatalysts to produce H_2 by photoreformation.

Metal chalcogenides appeared as efficient photocatalysts because of their small band gaps, which produce visible light activity. The higher electronic energy states in comparison to oxides facilitate the reduction of conduction band photoexcited electrons (Peng et al. 2016). CdS is used to facilitate H_2 generation due to its relatively negative conduction band energy in comparison to proton reduction (Fig. 4b) (Zhao et al. 2020). H_2 generation from glycerol and ascorbic acid using Pt/CdS as a photocatalyst composite has recently been explored (Bastos et al. 2014; Zhou et al. 2015), while surface layer formation on ZnS has proven advantageous for continuous formic acid reforming (Wang et al. 2014). Nevertheless, use of porous metal organic frameworks (MOFs) like UiO-66 could resist Cd^{2+} leaching (Shen et al. 2015; Zhou et al. 2015). Photoreforming of lactic acid has been studied using metal sulfide composites such as MoS_2-CdS, CdS, and NiS-CdS microstructures embedded with Te microspheres (Hu et al. 2015). Solid mixtures of Zn and Cd sulfide composites with Zn/Cd ratio 0.4:0.6 ($Cd_xZn_{1-x}S$) have also shown adjustable band gaps for H_2 production by photoreforming (Kozlova et al. 2014; Lopes et al. 2015). Similarly, ZnS-Bi_2S_3 nanoparticle composites accumulated on ZnO nanotubes on graphene have shown efficiency in glycerol photoreforming (Xitao et al. 2014). $CuInS_2$ has recently been used in the photoreforming of ethanol (Li et al. 2015a), while quaternary chalcogenides like $AgInZn_7S_9$ are gaining significance due to the possibility of controlled band gaps, facilitating photocatalytic H_2 production (Peng et al. 2015b). Surface amendments of CdSe nanoparticles with suitable pendant groups having attached carboxylate moieties reduces their water-solubility, while addition of Ni or Co to the resulting colloid make the systems highly efficient to produce H_2 from ascorbic acid (Das et al. 2013; Gimbert-Suriñach et al. 2014; Han et al. 2015, 2012; Wang et al. 2015b).

Highly porous crystalline metal and organic frameworks (MOFs and COFs) have been extensively studied in the last decade due to their high semiconducting properties (Fig. 4c, d) (Bavykina et al. 2020; Stegbauer et al. 2014). MOFs offer a potential platform for photocatalytic formation of H_2 due to their structural tunability and regularity, where H_2 productivity is equivalent to the transmission efficiency of photogenerated electrons. Cu-MOF shows more facile reduction to produce H_2 at a photocatalytic rate of 18.96 μmol h^{-1} due to its more negative conduction band compared to Cd-MOF (Song et al. 2017). A series of bifunctional FeX@Zr_6-Cu ($X = Cl^-$, Br^-, BF_4^-, and AcO^-)-functionalized MOFs exhibited high efficiencies to generate H_2 with a turnover number (TON) up to 33,700 h^{-1} due to the increase in H_2 productivity (Pi et al. 2020). Stegbauer et al. explored photoactive COFs through the synthesis of 1,3,5-tris-(4-formyl-phenyl)triazine (TFPT)-COF for photocatalytic H_2 production (Stegbauer et al. 2014). Thiazolo[5,4-*d*]thiazole (TpDTz)-COF enabled long-term (70 h) H_2 production with a productivity of 941 μmol h^{-1} g^{-1} (Biswal et al. 2019).

Nanocarbon materials and N- or P-doped semiconducting graphene (g-C_3N_4) are considered efficient, metal-free catalysts for the photoreforming process (Latorre-Sánchez et al. 2013; Liu et al. 2015b; Xiang et al. 2015; Ye et al. 2015). Light-harvesting poly(3-hexylthiophene) amended electron mediator g-C_3N_4 composites and Pt co-catalyst have shown high H_2 production efficiency from aqueous ascorbic acid (Zhang et al. 2015b). The catalytic Pt/g-C_3N_4 platform resulted in hydrogen production from wastewater under visible light through consumption of H_2O_2 by sacrificial macrolide antibiotics (Xu et al. 2017). Incorporation of co-catalysts, such as metal oxide nanoparticles and gold nanoparticles, on a semiconductor can enhance the efficiency of photoreforming (Serra et al. 2015; Xu and Xu 2015). Photocatalysis is attributed to various factors, including light-blocking, controlled substrate oxidation over semiconductor surfaces, and electron–hole rearrangement on disproportionate co-catalyst. The rate of light-stimulated H_2 generation on Pd/TiO_2 from aqueous MeOH is controlled by the availability of the perimeter across the interface of co-catalyst and semiconductor surface. According to Bowker et al. charge transfer processes including the adsorbed substrate preferentially occur at the interface of metal-support, which becomes more abundant upon increased metal loading. At an optimum concentration, the particles merge with reduced-perimeter (Al-Mazroai et al. 2007). The elements Cu (Petala et al. 2015), Ni (Chen et al. 2015b;

Fujita et al. 2016), Fe (Cao et al. 2015d), and Co (Mahoney et al. 2015) have recently been explored to develop economical co-catalysts. Nanoparticles based on transition metal phosphide cocatalysts have gained attention for H_2 production in light-triggered systems (Yue et al. 2015). Co_2P- and Ni_2P-loaded CdS nanorods are highly efficient at producing H_2 from mandelic and lactic acids (Cao et al. 2015a, 2014, 2015c). $Co_{0.85}Se$ and Ni_2B supported on Se were recently found to be promising co-catalysts for inexpensive H_2 evolution by a photoreforming approach (Cao et al. 2015b; Wang et al. 2015c). RGO/CdS and RGO/TiO_2 composites have also been found to be effective for H_2 production by photocatalysis from lactic acid/water or water/ethanol solutions (Babu et al. 2015; Nagaraju et al. 2015).

Biomass feedstocks have enormous potential to provide useful oxygenates for strategic conversion of bio-based wastes to H_2 energy through biomass valorization (Taipabu et al. 2022). Lignocellulosic materials are most abundant as plant mass, which can be obtained from forest products (wood or shrubs), agricultural offshoots (wheat straw, rice husks, or corn hobs), energy-based plants (water hyacinth or sorghum), and various urban and industrial waste materials (Dahmen et al. 2019). Crops supplying starch/sugar and vegetable oil are also advantageous for generating H_2 due to the presence of hydrogen-rich polysaccharides and long chain fatty acids (LCFAs), respectively (Salama et al. 2019; Sołowski et al. 2018). Biomass-derivatives are composed of various oxygen-enriched functional groups including acetals, carbonyls (aldehydes and ketones), carboxylic groups, ethers, and hydroxyl (alcohols, phenols, and polyols) (Wu et al. 2016). Various biomass-derived potential substances like alcohols, aldehydes, polyols, ketones, saccharides, and carboxylic acids play a key role in producing H_2 by photoreforming of biomass feedstocks (Table 2). Thus, various renewable waste-derived feedstocks can produce H_2 at high rates, opening an opportunity for waste valorization.

3 Hydrogenogenic fermentation for evolution of hydrogen

Fermentative biohydrogen is considered a potential contender for many conventional energy sources due to its environmentally friendly nature, which lessens fossil fuel consumption and pollution control measures (Ahmed et al. 2021). There are two fermentative processes that can yield H_2: dark fermentation (anaerobic hydrogenogenic acidogenic fermentation) and photo-fermentation. These technologies have the potential to become cost competitive as they can use low-value waste biomasses as feedstock (Jiao 2021). The dark fermentation pathway is light-independent and performs heterotrophic fermentation using facultative or obligate anaerobic microbes (Basak et al. 2020; Chang et al. 2018). In this process, hydrogenogenic microorganisms anaerobically utilize solid/soluble organic matter from low-cost organic wastes and municipal/industrial wastewater producing gas mixture (*i.e.*, H_2, CO_2) and various byproducts including volatile fatty acids (VFAs), ethanol, acetone, propanol, and butanol (Eqs. 7–12) (Wang and Yin 2021; Zhou et al. 2018). The yields of H_2 vary depending on the fatty acid pathway and the type of sugar present in the waste biomasses (e.g., glucose, sucrose, xylose) (Sarangi and Nanda 2020).

$$C_5H_{10}O_5 + 3.33H_2O \rightarrow 1.67C_2H_4O_2 + 1.67CO_2 + 3.33H_2 \quad (7)$$

$$C_5H_{10}O_5 + 1.67H_2O \rightarrow 0.83C_4H_8O_2 + 1.67CO_2 + 1.67H_2 \quad (8)$$

$$C_6H_{12}O_6 + 2H_2O \rightarrow 2C_2H_4O_2 + 2CO_2 + 4H_2 \quad (9)$$

$$C_6H_{12}O_6 \rightarrow C_4H_8O_2 + 2CO_2 + 2H_2 \quad (10)$$

$$C_6H_{12}O_6 + H_2O \rightarrow C_2H_6O + C_2H_4O_2 + 2CO_2 + 2H_2 \quad (11)$$

$$C_{12}H_{22}O_{11} + H_2O \rightarrow 2C_4H_8O_2 + 4CO_2 + 4H_2 \quad (12)$$

Substrates such as polysaccharidic waste biomasses, which are rich in glucose, sucrose, starch, cellulose, and lignocellulose, are considered suitable for dark fermentation due to their conversion efficiency to hydrogen and low cost to enhance hydrogen productivity by minimizing the process cost (Chen et al. 2006; Nasr et al. 2015; Reaume 2009). However, the complex structure of waste biomasses requires an efficient pretreatment process before fermentation to create microbial accessibility to fermentable sugars (Saha et al. 2016). Dark fermentation involves converting complex organic matter into simpler products through hydrolysis and acidogenesis

Table 2 Photocatalytic H_2 production from various biomass-derived oxygenates via photoreformation

Reaction medium	Photocatalyst	Source of light	P/W (I/mW cm^{-2})	Temperature (°C)	H_2 productivity (μmol g_{cat}^{-1} h^{-1})	References
H_2O/MeOH (v, 9:1)	Pt (1%) + TiO_2	Xe	300	–	10,860	Wang et al. (2015a, b, c)
H_2O/MeOH (v, 7:3)	Pt (1%)/$^{P25}TiO_2/SiO_2$	Solar simulator	100	280	571,000	Han and Hu, (2015)
		Solar simulator (> 420 nm)			497,000	
MeOH (aq, 2.5 M)	Pt (1%)/(CNT + TiO2)	Hg	150	25	1380	Silva et al. (2015)
Glucose (aq, 0.02 M)					99	
Fructose (aq, 0.02 M)					51	
Cellobiose (aq, 0.02 M)					79	
Arabinose (aq, 0.02 M)	Pt(1%)/TiO_2 (anatase)				105	
H_2O/MeOH (v, 1:1)	Pt (0.5%)/TiO_2/CNT (10%) (nanofibers)	Hg	200	–	40,600	Moya et al. (2015)

Table 2 (continued)

Reaction medium	Photocatalyst	Source of light	P/W (I/mW cm^{-2})	Temperature (°C)	H_2 productivity (μmol g_{cat}^{-1} h^{-1})	References
H_2O/MeOH (v, 9:1)	Au (1.5%)/$^{P25}TiO_2$	UV (365 nm)	6.5	–	13,500	Chen et al. (2015a)
	Au (1.5%)/TiO_2 (anatase)				8500	
	Au (1.5%)/TiO_2 (brookite)				6700	
	Au (1.5%)/TiO_2 (rutile)				900	
H_2O/EtOH (v, 9:1)	$^{P25}TiO_2$				1300	
	Au (1.5%)/$^{P25}TiO_2$				9800	
	Au (1.5%)/TiO_2 (anatase)				7300	
	Au (1.5%)/TiO_2 (brookite)				4900	
	Au (1.5%)/TiO_2 (rutile)				400	
	Au (0.5%)/$H_2Ti_3O_7$ (nanotubes)				200	
	Au (0.5%)/TiO_2 (rutile)				400	
	Au (0.5%)/TiO_2 (anatase nanotubes)				31,800	
	TiO_2 (anatase nanotubes)				900	
	Au (1.5%)/$^{P25}TiO_2$				32,200	
H_2O/glycerol (v, 9:1)	$^{P25}TiO_2$				1900	
	Au (0.5%)/$^{P25}TiO_2$				27,900	
	Au (0.5%)/TiO_2 (anatase)				15,000	
	Au (0.5%)/TiO_2 (brookite)				13,800	
	Au (0.5%)/TiO_2 (rutile)				3200	
	Au (0.5%)/TiO_2 (anatase nanotubes)				29,200	
H_2O/ethylene glycol (v, 9:1)	Au (1.5%)/$^{P25}TiO_2$				20,900	
	Au (1.5%)/TiO_2 (anatase)				12,000	
	Au (0.5%)/TiO_2 (anatase nanotubes)				22,700	
	Au (1.5%)/$^{P25}TiO_2$				23,100	

Table 2 (continued)

Reaction medium	Photocatalyst	Source of light	P/W (I/mW cm^{-2})	Temperature (°C)	H_2 productivity (μmol g_{cat}^{-1} h^{-1})	References
H_2O/MeOH (v, 10:1)	Au (Au/Ti = 0.017) @ TiO_2 (nanotubes)	Xe (> 400 nm)	100	–	482	Yang et al. (2015)
	Au (Au/Ti = 0.015) @ TiO_2 (nanotubes)				223	
H_2O/MeOH (v, 3:1)	Au (0.9%)/$^{P25}TiO_2$	Solar simulator	1000	35	7010	Serra et al. (2015)
H_2O/MeOH (v, 3:1)	RGO/TiO_2	Xe–Hg	300	25	1200	Nagaraju et al. (2015)
H_2O/MeOH (v, 4:1)	TiO_{2-x}	Xe (> 420 nm)	750	–	36	Jiang et al. (2015b)
H_2O/MeOH (v, 9:1)	ZnO	Xe	300	Room temperature	30,000	Guo et al. (2015)
H_2O/formaldehyde (v, 9:1)					33,750	
H_2O/EtOH (v, 20:1)	Pt (1%)/TiO_2 (anatase)	UV (> 365 nm)	2	–	3630	Bashir et al. (2015)
EtOH (96%)	Pt (0.2%)/TiO_2 (anatase/brookite)	Solar simulator	150	25	930	Romero Ocaña et al. (2015)
EtOH (aq, 7.34 M)	Pt (2.1%)/TiO_2	UV 300–400 nm	12 × 15	–	11,074	López et al. (2015)
Glycerol (aq. 7.34 M)					6335	
Ethylene glycol (aq, 7.34 M)					7565	
H_2O/EtOH (v, 1:4)	$^{P25}TiO_2$	UV	6.5	–	1200	Chen et al. (2015b)
H_2O/EtOH (v, 1:19)	Ni (0.5%)/$^{P25}TiO_2$				24,000	
H_2O/EtOH (v, 1:4)	Au (2%)/$^{P25}TiO_2$				32,400	
H_2O/EtOH (v, 9:1)	Ag-Fe–Ni/TiO_2	Xe	500	30	794	Sun et al. (2015)
H_2O/EtOH (v, 4:1)	$CuInS_2$(2.5%)/$^{P25}TiO_2$	Xe	300	–	273	Li et al. (2015a, b)
H_2O/EtOH (v, 1:1)	$SrTiO_3$	Hg	500	–	95	Peng et al. (2015a, b)
H_2O/glycerol (v, 30:1)	Pt (1%)/$^{P25}TiO_2$	Xe (> 320 nm)	300	10	4280	Jiang et al. (2015a, b)
Glycerol (aq, 1 M)	CuO (0.4%)/$^{P25}TiO_2$	Xe	250	–	863	Petala et al. (2015)
Glycerol (aq, 0.1 M)	Cu_2O/$^{P25}TiO_2$	Xe (> 420 nm)	1.5	–	240	Kum et al. (2015)
H_2O/glycerol (v, 9:1)	Cu (10% mol)/TiO_2	Halogen	500	24	5772	Bashiri et al. (2015)
H_2O/glycerol (v, 19:1)	Cu (1.5%)/TiO_2 (nanorods)	Sunlight	–	–	50,339	Praveen Kumar et al. (2015)
	TiO_2 (nanorods)				2950	
	$^{P25}TiO_2$				2100	

Table 2 (continued)

Reaction medium	Photocatalyst	Source of light	P/W (I/mW cm^{-2})	Temperature (°C)	H_2 productivity (μmol g_{cat}^{-1} h^{-1})	References
H_2O/glycerol (v, 9:1)	NiO (2%)/TiO_2 (anatase/rutile, 7:3)	Hg	500	50	1230	Fujita et al. (2016)
	CuO (2%)/TiO_2 (anatase/rutile, 7:3)				1370	
	CoO (2%)/TiO_2 (anatase/rutile, 7:3)				660	
H_2O/glycerol (v, 19:1)	RGO (3%)/TiO_2	Hg	250	–	8226	Babu et al. (2015)
	Cu_2O (1%)/TiO_2				16,653	
	RGO (3%)-Cu_2O (1%)/TiO_2				110,968	
H_2O/glycerol (v, 19:1)	ZnO (nanorods)/RGO (12%)	Xe	300	Room temperature	92	Lv et al. (2015)
H_2O/glycerol (v, 1:1)	Bi_2WO_6	Xe	300	–	7400	Panmand et al. (2015)
H_2O/glycerol (v, 9:1)	ZnS/ZnO (nanotube arrays)	Xe	350	25	384	Bao et al. (2015)
	ZnS				232	
	ZnO (nanotube arrays)				38	
Glycerol (aq, 1.368 M) + 1 M NaOH	Pt (0.5%)/$Cd_{0.5}Zn_{0.5}S$	Hg (> 420 nm)	250	–	630	Peng et al. (2016)
Glycerol (v, 1:1) + 1.5 M NaCl	Pt/$Cd_{0.6}Zn_{0.4}S$:(γ-Zn$(OH)_2$)	Hg–Xe (> 418 nm)	500	–	239	Lopes et al. (2015)
H_2O/formaldehyde (v, 7:1)	Cu (Fe/Cu = 4)/$LaFeO_3$	Xe (> 400 nm)	125	–	343	Li et al. (2015b)
H_2O/lactic acid (v, 7:3)	Pt (5%)/$TaO_{2.18}Cl_{0.64}$	Xe	300	–	1500	Tu et al. (2015)
H_2O/lactic acid (v, 7:1)	Ce (4% mol): Sb (10%): SnO_2	Xe (> 320 nm)	300	–	8.5	Liu et al. (2015a, b)
H_2O/lactic acid (v, 9:1)	MoS_2 (2.5%)/CdS	Xe (> 420 nm)	350	–	543	Lang et al. (2015)
	Pt (0.25%)/CdS				450	
	RGO-MoS_2(2.5%)/CdS				621	
H_2O/lactic acid (v, 20:3)	CdS + $Co_{0.85}Se$ (5%)/RGO-PEI (PEI: poly(ethyleneimine)	LED (> 420 nm)	30 × 3	–	17,600	Cao et al. (2015b)
	Pt (0.1%)/CdS				18,600	
H_2O/lactic acid (v, 9:1)	Ni_xB (0.8%)/CdS	Xe (> 420 nm)	180	–	4800	Wang et al. (2015a, b, c)
H_2O/lactic acid (v, 19:1, pH 3) + NaOH	CoP + CdS	LED (> 420 nm)	30 × 3	Room temperature	202,800	Cao et al. (2015c)
	Ni_2P + CdS				143,600	
	Cu_3P + CdS				77,600	
H_2O/lactic acid (v, 10:1)	MoP (16.7%)/CdS (nanorods)	visible (> 420 nm)	–	–	163,200	Yue et al. (2015)

Table 2 (continued)

Reaction medium	Photocatalyst	Source of light	P/W (I/mW cm^{-2})	Temperature (°C)	H_2 productivity (μmol g_{cat}^{-1} h^{-1})	References
H2O/lactic acid (v, 9:1)	NiS (9%)-CdS (37%)/Te	Xe (> 420 nm)	300	–	317	Hu et al. (2015)
	Pt (11%)-Pd (15%)/CdS (31%)/Te				236	
H_2O/lactic acid (v, 9:1)	MoS_2 (1.5%)/CdS/UiO-66 (50%) (UiO-66: poly-Zr–benzenedicarboxylate MOF)	Xe (> 420 nm)	300	–	32,500	Shen et al. (2015)
Glycerol	Pt-$Bi_2Ti_2O_7$	UV	–	–	41.4	Musso et al. (2023)
Ethanol (v, 10%)	Ni/Urea-CN	Fluorescent lamp	~ 5	Room temperature	760.5	Gunawan et al. (2022)
H_2O/Glycerol (v, 10%)	Au/TiO2@n-octadecane	Xe lamp	35	–	5444	Zhong et al. (2022)
H_2O/glycerol (v, 14%)	Pt@UiO-66(Zr)-NH_2	Solar simulator	230	–	766.67	Rueda-Navarro et al. (2022)
Formaldehyde	g-C_3N_4	LED lamp (400–800 nm)	12.5	–	204.44	Munusamy et al. (2022)
Glucose	$Ni_{0.05}Au_{0.45}$/ TiO_2	Visible light	–	–	6391.86	Eqi et al. (2022)
H_2O/ethanol (v, 80:20)	FeOSnS/PdO_x/MnO_x	Hg lamp	4.4	–	546,000	Etemadi et al. (2022)
Glucose (aq, 5.3 mM)	Pt (0.5%)/$^{P25}TiO_2$	UVA (366 nm)	15 × 4	–	357	Speltini et al. (2015)
H_2O/olive mill wastewater (v, 3.3%)					183	
					342	
		Solar simulator	25		20	
Municipal wastewater	Au (0.5% mol)/TiO_2	Sunlight	–	–	22	Malato et al. (2016)

by producing short- and medium-chain fatty acids (SCFAs-MCFAs) and gaseous hydrogen (Fig. 5) (Chang et al. 2018). Several microorganisms harbor various hydrogenase enzymes (such as [FeFe]-hydrogenase, [NiFe]-hydrogenase, and [NiFeSe]-hydrogenase), which stimulate production and recycling of hydrogen under an anaerobic environment (de Sá et al. 2011). Among these enzymes, only [FeFe]-hydrogenase catalyzes hydrogen production, while the other two utilize produced hydrogen and are often found in hydrogen-consuming microorganisms. Comparatively higher expression of [FeFe]-hydrogenase (around 100-fold) than [NiFe]-hydrogenase in strict and facultative bacteria allows production of enough hydrogen during dark fermentation (Sołowski et al. 2018). *Clostridia*, *Escherichia coli*, *Enterobacter*, *Citrobacter*, *Alcaligenes*, and *Bacillus* strains of Gram-positive or Gram-negative bacteria are dominant in fermenters or digesters under strict or facultative anaerobic environments (Ferraren-De Cagalitan and Abundo 2021). Metabolic pathways and substrate diversity studies revealed the dominance of *Clostridium* species in dark fermentation utilizing a wide variety of substrates for the production of H_2 (3.94 mol H_2 mol^{-1} hexose − 5.42 mol H_2 mol^{-1} carboxymethylcellulose) through acetate, butyrate, and propionate pathways (Wang and Yin 2021).

Production of hydrogen reached the maximum of 1.5 mol H_2 mol^{-1} of fructose and 1.3 mol H_2 mol^{-1} of sucrose when *Firmicutes* dominant anaerobic consortium from brewery wastewater was used as inoculum (Pachiega et al. 2019). Here, the yield of

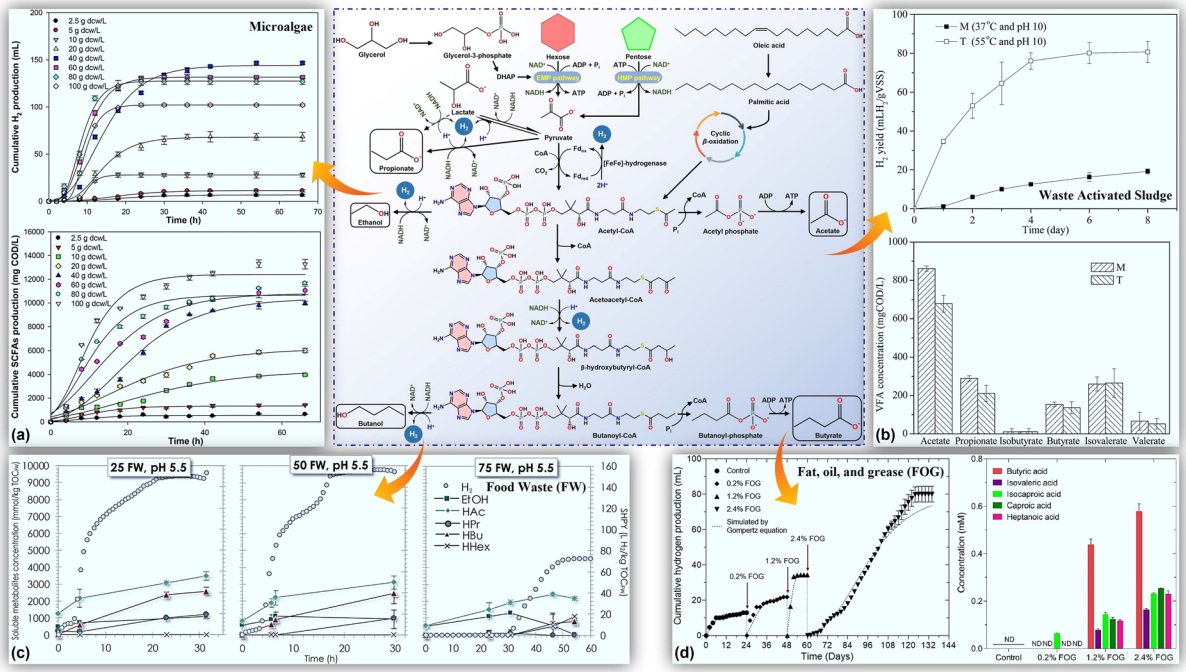

Fig. 5 Metabolic pathways involved in dark fermentation of complex organic substrates such as microalgae (**a**), waste activated sludge (**b**), food waste (**c**), and fat, oil, grease (**d**) to produce hydrogen, short- and medium-chain fatty acids, ethanol, and butanol (Akhlaghi et al. 2019; Elsamadony et al. 2021; Saha et al. 2019; Wan et al. 2016; Wang and Yin 2021; Yun et al. 2016)

hydrogen depends on specific parameters such as substrate type, loading rate, system pH and temperature, microbial adaptability to specific substrate, inoculum-to-substrate ratio, and concentrations of various additives in the fermentation broth (Akhlaghi et al. 2019; Li et al. 2021; Ren et al. 2022; Saha et al. 2020). An increase of microalgal loading as fermentation substrate to 40 g dry cell weight L^{-1} in mesophilic dark fermenters achieved a maximum hydrogen yield of 36 mL H_2 g^{-1} through the acetate pathway, which decreased upon further loading (Fig. 5a) (Yun et al. 2016). Around a 13% decrease in the hydrogen yield occurred when sucrose was the primary substrate compared to fructose (1.5 mol H_2 mol^{-1}) (Pachiega et al. 2019). *Clostridium acetobutylicum* produced 63 ml H_2 g^{-1} starch in solid state (total solid: 20%) dark fermentation of ground wheat (Ozmihci 2017). Use of waste activated sludge in thermophilic (55 ℃) reactors produced 317% higher hydrogen yield at pH 10 over mesophilic (37 ℃) reactors (Fig. 5b). However, VFA production (especially, acetate and propionate) was much higher in the mesophilic reactors (Wan et al. 2016). Production of hydrogen (3.8 mol H_2 mol^{-1} of sugar) reached its theoretical yield (4 mol H_2 mol^{-1} of glucose) during hyperthermophilic fermentation of fruit and vegetable waste using the halophilic bacterium *Thermotoga maritima* (Saidi et al. 2018). Acidogenic dark fermentation of food waste (FW) at an inoculum-to-substrate ratio of 50:50 produced 160 L H_2 kg^{-1} TOC_{FW} during mesophilic operation at pH 5.5 (Fig. 5c) (Akhlaghi et al. 2019). Incorporation of ryegrass into sewage sludge fermentation increased the final hydrogen yield (60 mL g^{-1} VS) by five times at a ratio of 30:70 compared to the yield in sludge alone (Yang and Wang 2017). Thus, the hydrogen productivity varies depending on substrate variations and fermentation conditions.

Acclimatization of the microbial inoculum to enrich the hydrogenogenic bacterial population improved the conversion of specific substrates to hydrogen. Hydrogen yield was boosted to 19.5 L H_2 L^{-1} in thin stillage using acclimatized anaerobic digester sludge due to enrichment of acidogenic *Clostridium acetobutyricum*, *Klebsiella pneumonia*,

Clostridium butyricum, and *Clostridium pasteurianum*, which improved the specific hydrogen production rate (3.5 times higher than with unacclimatized sludge) (Nasr et al. 2011). Bioaugmentation with *Clostridium thermocellum* improved hydrogen yield by 96.80% in thermophilic fermentation of paper sludge through increase of holocellulose degradation rate (32.95%) (An et al. 2018). The presence of active acidogenic bacteria belonging to the phyla *Firmicutes* and *Bacteroidetes* in the acclimatized inoculum improved the hydrogen yield by 48% compared to its unacclimatized counterpart (Chang et al. 2018). Cellobiose-acclimatized sewage sludge enriched the population of genus *Clostridium* as a main hydrogen producer and produced 2.08 mmol H_2 g^{-1} filter paper (Ho et al. 2012). Enrichment of iron-dependent hydrogenases expressing *Anaerofilum* sp. in the bioreactors enhanced the hydrogen yield to 13.64 mmol in five months of operation (Venkata Mohan et al. 2011). A combination of various additives such as zero-valent iron, nano zero-valent iron, Ni^0 nano particles, and biochar stimulated the acidogenesis process through the activation of various hydrogenases to achieve hydrogen yields near the theoretical potential of the substrate (Mohd Jamaludin et al. 2023; Ren et al. 2022). Metallic additives improved enzymatic activities through oxidation/reduction to promote hydrogen production (Saha et al. 2020). Upon addition to fermentation reactors, zero-valent metals oxidize in the aqueous phase and promote the synthesis and activity of major enzymes such as hydrogenase and ferredoxin (Taherdanak et al. 2015). Shifting of a microbial population toward *Clostridium* occurred upon addition of Fe^{2+} ions in grass-fermenting reactors, which enhanced the hydrogen yield (72.8 mL g^{-1} dry grass) by 49.6% (Yang and Wang 2018a). Fe^0 nanoparticles at a concentration of 400 mg L^{-1} increase the hydrogen production rate and yield by 128% and 73%, respectively, by shortening the lag period and facilitating substrate hydrolysis and utilization through the enrichment of *Clostridium* sp. (Yang and Wang 2018b). Fe^0 nanoparticle supplementation in dark fermentation improved the hydrogen yield to 20 mL H_2 g^{-1} VS of microalgae (6.5 times higher than the control) by enriching the populations of *Clostridium* and *Terrisporobacter* sp. (Yin and Wang 2019).

Addition of magnetite at a concentration of 100 mg L^{-1} induced the growth of acidogenic bacteria such as *Sporolactobacillus*, *Clostridium*, and Coprothermobacter, which increased the hydrogen production by 46% (Gökçek et al. 2023). Magnetite nanoparticles embedded in granular activated carbon (GAC) improved the hydrogen productivity rate in dark fermentation by 63.99% compared to non-magnetite GAC (Mohd Jamaludin et al. 2023). The high specific surface area and porosity of biochar act as a support matrix to microbial attachment, growth, and cellular vitality and improve syntrophic interspecies interactions, further expediting the holistic conversion of substrate to fermentative products. Use of granular activated carbon as a support matrix for biofilm development enhanced the hydrogen yield of 1.77 mol H_2 mol^{-1} $substrate_{consumed}$ during thermophilic dark fermentation (Jamali et al. 2016). Biofilm formation on the surface of biochar during co-culture of *Enterobacter aerogenes* and *E. coli* in fermentation of municipal solid waste maximized the hydrogen yield to 96.63 ml H_2 g^{-1} $carbohydrate_{initial}$ by accelerating COD removal (53%) and shortening the lag phase from 12.5 h to 8.1 h (Sharma and Melkania 2017). Supplementation of sugarcane bagasse-derived biochar improved hydrogen production (84.58 mL) by enhancing the hydrogen productivity (> 74%) of *Ethanoligenens harbinense* (Li et al. 2021). The synergistic effect of combining biochar and Fe^0 nanoparticles at concentrations of 600 mg L^{-1} and 400 mg L^{-1}, respectively, enhanced the hydrogen yield to 50.6 mL g^{-1} dry grass and shortened the lag phase by accelerating enriched *Clostridium*-mediated hydrolysis and fermentation (Yang and Wang 2019). Addition of zero-valent iron-activated carbon to wastewater sludge fermentative reactors improved the hydrogen yield (1.33 mol H_2 mol^{-1} glucose) by 50% through enrichment of the *Clostridium* spp. population (Zhang et al. 2015a). The synergistic impact of biochar (621 mg L^{-1}) and Ni^0 nanoparticle (17.2 mg L^{-1}) in dark fermentation increased the hydrogen production rate (558 mL h^{-1}) and hydrogen yield (237 mL g^{-1}) by decreasing the lag phase to 4.82 h (Sun et al. 2019a). Thus, a combination of metallic additives as co-factor for hydrogenases and biochar improved the microbial enzymatic activities through induction of electron transport among syntrophic partners and enriched the hydrogenogenic bacterial population in acidogenic fermenters for improved hydrogen production from organic biomass.

Utilization of lipidic waste such as FOG (fat, oil, grease) in dark fermentation produced a large amount of hydrogen from saturated and unsaturated LCFAs along with C4–C7 carboxylates through carboxylic chain elongation of SCFAs (Fig. 5d) (Saha et al. 2019). β-Oxidation of saturated (e.g., stearic acid, palmitic acid, myristic acid) and unsaturated (linoleic acid, linoelaidic acid, oleic acid) LCFAs during anaerobic fermentation generated C2 carboxylate and H_2 as an electron acceptor (Eq. 13) (Cavaleiro et al. 2016; Elsamadony et al. 2021). These C2 carboxylate and H_2 play a major role in the thermodynamic feasibility of the β-oxidation pathway, which demands a low hydrogen partial pressure of 1 Pa and acetate concentration of 8 or 9 mmol l^{-1} in the reactors (Saha et al. 2020). Failing to retain these conditions led to accumulation of saturated LCFA (palmitic acid, ~90%) in the fermenters as a major intermediate of the degradation pathways of the longer chain unsaturated LCFAs (Saha et al. 2019). Palmitic acid and myristic acid emerged as the main intermediates of the monounsaturated LCFAs degradation in the absence of methanogenic activity, leading to their accumulation in the reactors (Cavaleiro et al. 2016). Syntrophic coupling among acidogenic LCFA-degrading bacteria with acetate-utilizing and hydrogenotrophic microorganisms help sustained an optimum environment to facilitate continuous β-oxidation (Cavalcante et al. 2017). The occurrence of reverse metabolic traits is feasible in the presence of energy-rich, reduced compounds such as ethanol and lactate to provide energy and reduce equivalents and acetyl-CoA during the anaerobic reactor microbiome-mediated β-oxidation (Fig. 5) (Spirito et al. 2014). Various MCFAs such as C4–C6 carboxylates are the products of secondary anaerobic fermentation of SCFAs after acidogenic fermentation, where ethanol acts as an electron donor for carboxylic acid chain elongation/reverse β-oxidation (Eqs. 14 and 15) (Angenent et al. 2016; Cavalcante et al. 2017).

$$n\mathrm{CH_3(CH_2)_nCOOH} + n\mathrm{H_2O} \rightarrow \mathrm{CH_3(CH_2)_{n-2}COOH} + n\mathrm{C_2H_4O_2} + n\mathrm{H_2} \quad (13)$$

$$5\mathrm{C_2H_6O} + 3\mathrm{C_2H_4O_2} \rightarrow 4\mathrm{C_4H_8O_2} + 3\mathrm{H_2O} + 2\mathrm{H_2} \quad (14)$$

$$12\mathrm{C_2H_6O} + 3\mathrm{C_2H_4O_2} \rightarrow 5\mathrm{C_6H_{12}O_2} + 8\mathrm{H_2O} + 4\mathrm{H_2} \quad (15)$$

Syntrophic cooperation among ruminal mixed microbiome and cellulose-converting *Clostridium kluyveri* produced valeric and caproic acids in the presence of ethanol (Weimer et al. 2015). Anaerobic fermentation of municipal solid waste in a two-stage system consisting of an acidification and a chain elongation reactors achieved caproate production of 12.6 g l^{-1}, the highest among MCFAs (Grootscholten et al. 2014). A MCFA yield of 67% was obtained during anaerobic fermentation of wine lees (settled yeast cells and ethanol) using acclimatized inoculum along with hydrogen (45% of produced biogas), which primarily consists of caprylate and caproate at 36% each (Kucek et al. 2016b). Production of hydrogen (3000 ppm) occurred in an anaerobic up-flow bioreactor producing caprylate (0.33 g L^{-1} h^{-1}) as a major MCFA when ethanol and acetate were used as feedstocks (Kucek et al. 2016a). The thermodynamic feasibility of MCFA production in dark fermentation is highly supportive due to presence of a secondary by-product (ethanol), and it promoted the growth and syntrophic relationship among *Clostridium kluyveri* and ethanol-producing bacteria to facilitate the production of 10–20% more hydrogen with MCFA (especially, caproate) (Ding et al. 2010). Thus, conversion of organic biomass in dark fermentation could lead to the production of various value-added chemicals and increase hydrogen yield through the induction of microbial metabolic syntrophy.

4 Techno-economic assessment of hydrogen technologies

The sustainable production of hydrogen is of prime importance for its commercialization as a fuel. A competitive and reasonable price of hydrogen fuel can be achieved through increased rate of production and reliability of processing (Godvin Sharmila et al. 2022). There are several key drivers that mainly influence the green hydrogen economy, *i.e.*, (a) cost of substrate/feedstock and pretreatment, (b) cost of the hydrogen production system, (c) cost of downstream processing for purification of hydrogen, (d) cost of transportation and storage, and (e) cost of distribution (Lane et al. 2021; Prabakar et al. 2018). The physicochemical processes for production of hydrogen are highly efficient with respect to productivity and purity; however, the economic viability of these

processes is low due to their high energy requirements (Godvin Sharmila et al. 2022). Various technologies have been developed and tested for commercial hydrogen production. The chemical processes with broad industrial applications include water splitting by electrolysis, gasification of coal, and steam reforming, while biological processes include photobiological hydrogen production and dark fermentation (Brar et al. 2022; Mahmod et al. 2021; Qyyum et al. 2022). Among chemical pathways, electrolysis is widely employed, whereas steam reforming of methane is the most cost-effective method for hydrogen production, with a cost of US$ 7 GJ^{-1} (Kalamaras and Efstathiou 2013). The combination of electrolysis with a geothermal process for energy could cost around US$ 1.09 kg^{-1} (Yilmaz et al. 2019). The pyrolysis and gasification of biomass could generate hydrogen fuel at a cost of around US$ 8.9–15.5 GJ^{-1} and US$ 10–14 GJ^{-1}, respectively, which varies with the cost of raw materials (Balat and Balat 2009).

Biological processes are comparatively expensive because of applicability issues. The major bottlenecks include the high operational costs of bioprocessing, process instability, and low H_2 yields (Das and Basak 2021). For instance, hydrogen production via a photofermentation process costs around US$ 502.10 GJ^{-1}, which amounted to 90% of the total cost (Bhatia et al. 2021). One of the major hurdles in commercialization of hydrogen production through dark fermentation is the excessive cost of substrates (Yukesh Kannah et al. 2021). The cost of dark fermentative hydrogen production from glucose increased 5–10 times higher than that of photofermentation (US$ 2 kg^{-1} H_2) and indirect biophotolysis (US$ 1.42 kg^{-1} H_2) due to high cost of substrate, which consumed 88% of the production cost (Ahmed et al. 2021; Godvin Sharmila et al. 2022). The cost for bioprocessing can be significantly reduced if waste biomasses from industrial or agricultural sectors are utilized, since complex carbohydrates are available in massive quantities at comparatively cheaper prices. The waste-based hydrogen economy can overcome the largest electricity/energy barrier and encourage sustainable fuel production with greater energy security. The biomass substrate cost is highly subject to principal, operational, and maintenance costs, for levelled energy cost (LCOE) is less responsive to biohydrogen, which costs around US$ 7 kg^{-1} (Ahmed et al. 2021; Lee et al. 2008). Palm oil milling effluent is a by-product of the process and must be treated to meet environmental regulations. It can be utilized as a cost-effective feedstock for hydrogen production considering its low cost (Nurul-Adela et al. 2016). Hydrogen production through dark fermentation of food waste is inexpensive, US$ 0.814 kWh^{-1}, which provided an investment return of 29.8% within 7.2 years of the payback period (Cudjoe et al. 2022). The two-stage anaerobic technology is thought to be cost effective as its payback time is substantially shorter than its expected life (Mahmod et al. 2021).

Industrial effluents from dairy; slaughterhouse; and food and starch processing industries; and oil refineries also can be an effective feedstock for hydrogen production as it contains ample organic matter. A techno-economic study of hydrogen production using black liquor as a substrate via dark fermentation showed H_2 productivity of 12,450 m^3 $year^{-1}$ and annual revenue of US$ 35,481, with an initial investment payback period of 5.92 years (Tawfik et al. 2021b). Another study of H_2 and CH_4 generation from biscuit wastewater treatment via anaerobic digestion indicated payback periods of 5.7 and 7.1 years, respectively, although the initial investment for H_2 was 22% higher than that of CH_4 production due to more sophisticated processing (Tawfik et al. 2021a). These technologies achieved green energy production and industrialization with pollution prevention to address sustainable development goals (SDGs). The investment profits and payback period for hydrogenation of petrochemical industry wastewater under psychrophilic conditions were US$ 24,295 $year^{-1}$ and 7.13 years, respectively (Elreedy et al. 2019).

The world's biggest economies including USA, China, Japan, and India have encouraged investment in the development of hydrogen fuel (Lee et al. 2011). Among these four nations, China created the largest market for biohydrogen and has expected to reach the industry's output value to US$ 157.44 billion in 2025 (Koty 2022; Nakano 2022). Japan, USA, and India have started investment of around US$ 3.4, 8, and 25 billion, respectively to bring down the cost of green hydrogen to US$ 1 kg^{-1} by 2030 (Chaudhary 2022; DOE 2022; Nakano 2021). Such a large investment by these big economies will ensure state-of-the-art developments in biohydrogen infrastructures and technologies that will eventually produce more benefits than investment with better cost feasibility. The hydrogen economy significantly prevents pollution.

It has been estimated that utilization of hydrogen fuel instead of gasoline for more than 15 years can save ~ 29.9 million tonnes of CO_2-eq (Wulf and Kaltschmitt 2012). Moreover, the efficiency of diesel and hydrogen engines appears to be comparable (Stichnothe and Azapagic 2009). Therefore, employing hydrogen as a substitute fuel for conventional fossil fuels might significantly reduce GHG emissions. The future of hydrogen industry is bright as this green economy can play a key role in achieving SDGs by supporting eco-friendly technologies, instigating sustainable production methods, and conserving natural resources (Qyyum et al. 2022). The hydrogen economy fosters societal equity, promotes sustainable growth, and reduces environmental risk and resource requirements. Regulations supporting low carbon emissions or minimized CO_2 emission to overcome economic challenges should be employed (Prabakar et al. 2018). Development of novel technologies such as single-pot processes and integrated bioprocessing are necessary to reduce the costs of processing.

5 Concluding remarks and outlook

The feasibility of hydrogen production from various organic waste biomasses has been assessed through numerous thermochemical, photocatalytic, and biological processes over the past decades. Conversion of oxygenated biomass derivatives to green hydrogen through selective light-triggered reformation (photoreformation) at ambient conditions in the presence of active metallic photocatalysts has emerged as a sustainable method preferable to thermocatalytic degradation or gasification. The use of graphene-based carbonaceous photocatalysts and earth-abundant low-cost metals, such as Cu and Ni, could be advantageous to resist the photocorrosion of metal sulfides. Alternatively, dark fermentation has appeared as a potential contender due to its ability to produce multiple value-added chemicals along with hydrogen. Optimization of operational parameters such as substrate type, loading rate, system pH, temperature, microbial acclimatization to specific substrate, inoculum-to-substrate ratio, and concentrations of various additives (especially, Fe and Ni ions and biochar) in dark fermentation could improve the holistic conversion of organic wastes and simultaneous maximization of product yields. Upgrading produced hydrogen and downstream processing of value-added chemicals in the fermentation broth require substantial research to facilitate maximum energy recovery from organic wastes to ensure long-term sustainability. Thus, fostering eco-friendly technologies such as photoreformation and dark fermentation for hydrogen production from waste bioresources and promoting green energy utilization for prevention of environmental pollution could brighten the future of hydrogen industry.

Acknowledgements This work was supported by the Medicine-Engineering-Bio (MEB) research fund of Hanyang University, Seoul, Republic of Korea (HY-202000000002809).

References

Ahmed SF, Rafa N, Mofijur M, Badruddin IA, Inayat A, Ali MS, Farrok O, Yunus Khan TM (2021) Biohydrogen production from biomass sources: metabolic pathways and economic analysis. Front Energy Res 9:753878

Akhade SA, Singh N, Gutiérrez OY, Lopez-Ruiz J, Wang H, Holladay JD, Liu Y, Karkamkar A, Weber RS, Padmaperuma AB, Lee M-S, Whyatt GA, Elliott M, Holladay JE, Male JL, Lercher JA, Rousseau R, Glezakou V-A (2020) Electrocatalytic hydrogenation of biomass-derived organics: a review. Chem Rev 120(20):11370–11419

Akhlaghi M, Boni MR, Polettini A, Pomi R, Rossi A, De Gioannis G, Muntoni A, Spiga D (2019) Fermentative H_2 production from food waste: parametric analysis of factor effects. Bioresour Technol 276:349–360

Al-Mazroai LS, Bowker M, Davies P, Dickinson A, Greaves J, James D, Millard L (2007) The photocatalytic reforming of methanol. Catal Today 122(1):46–50

Alonso DM, Bond JQ, Dumesic JA (2010) Catalytic conversion of biomass to biofuels. Green Chem 12(9):1493–1513

An Q, Wang J-L, Wang Y-T, Lin Z-L, Zhu M-J (2018) Investigation on hydrogen production from paper sludge without inoculation and its enhancement by *Clostridium thermocellum*. Bioresour Technol 263:120–127

Angenent LT, Richter H, Buckel W, Spirito CM, Steinbusch KJJ, Plugge CM, Strik DPBTB, Grootscholten TIM, Buisman CJN, Hamelers HVM (2016) Chain elongation with reactor microbiomes: open-culture biotechnology to produce biochemicals. Environ Sci Technol 50(6):2796–2810

Babu SG, Vinoth R, Praveen Kumar D, Shankar MV, Chou H-L, Vinodgopal K, Neppolian B (2015) Influence of electron storing, transferring and shuttling assets of reduced graphene oxide at the interfacial copper doped TiO_2 p–n heterojunction for increased hydrogen production. Nanoscale 7(17):7849–7857

Bajracharya S, Sharma M, Mohanakrishna G, Dominguez Benneton X, Strik DPBTB, Sarma PM, Pant D (2016)

An overview on emerging bioelectrochemical systems (BESs): technology for sustainable electricity, waste remediation, resource recovery, chemical production and beyond. Renew Energy 98:153–170

Balat M, Balat M (2009) Political, economic and environmental impacts of biomass-based hydrogen. Int J Hydrogen Energy 34(9):3589–3603

Bao D, Gao P, Zhu X, Sun S, Wang Y, Li X, Chen Y, Zhou H, Wang Y, Yang P (2015) ZnO/ZnS heterostructured nanorod arrays and their efficient photocatalytic hydrogen evolution. Chem Eur J 21(36):12728–12734

Bartholomew CH, Farrauto RJ (2010) Fundamentals of industrial catalytic processes, 2nd edn. Wiley, Hoboken

Basak B, Saha S, Chatterjee PK, Ganguly A, Woong Chang S, Jeon B-H (2020) Pretreatment of polysaccharidic wastes with cellulolytic *Aspergillus fumigatus* for enhanced production of biohythane in a dual-stage process. Bioresour Technol 299:122592

Bashir S, Wahab AK, Idriss H (2015) Synergism and photocatalytic water splitting to hydrogen over M/TiO_2 catalysts: effect of initial particle size of TiO_2. Catal Today 240:242–247

Bashiri R, Mohamed NM, Kait CF, Sufian S (2015) Hydrogen production from water photosplitting using Cu/TiO_2 nanoparticles: effect of hydrolysis rate and reaction medium. Int J Hydrogen Energy 40(18):6021–6037

Bastos SAL, Lopes PAL, Santos FN, Silva LA (2014) Experimental design as a tool to study the reaction parameters in hydrogen production from photoinduced reforming of glycerol over CdS photocatalyst. Int J Hydrogen Energy 39(27):14588–14595

Bavykina A, Kolobov N, Khan IS, Bau JA, Ramirez A, Gascon J (2020) Metal-organic frameworks in heterogeneous catalysis: recent progress, new trends, and future perspectives. Chem Rev 120(16):8468–8535

Bernardo P, Drioli E, Golemme G (2009) Membrane gas separation: a review/state of the art. Ind Eng Chem Res 48(10):4638–4663

Bernardo P, Barbieri G, Drioli E (2010) Evaluation of membrane reactor with hydrogen-selective membrane in methane steam reforming. Chem Eng Sci 65(3):1159–1166

Bhatia SK, Jagtap SS, Bedekar AA, Bhatia RK, Rajendran K, Pugazhendhi A, Rao CV, Atabani AE, Kumar G, Yang Y-H (2021) Renewable biohydrogen production from lignocellulosic biomass using fermentation and integration of systems with other energy generation technologies. Sci Total Environ 765:144429

Biswal BP, Vignolo-González HA, Banerjee T, Grunenberg L, Savasci G, Gottschling K, Nuss J, Ochsenfeld C, Lotsch BV (2019) Sustained solar H_2 evolution from a thiazolo[5,4-*d*]thiazole-bridged covalent organic framework and nickel-thiolate cluster in water. J Am Chem Soc 141(28):11082–11092

Brar KK, Cortez AA, Pellegrini VOA, Amulya K, Polikarpov I, Magdouli S, Kumar M, Yang Y-H, Bhatia SK, Brar SK (2022) An overview on progress, advances, and future outlook for biohydrogen production technology. Int J Hydrogen Energy 47(88):37264–37281

Cao S, Chen Y, Wang C-J, He P, Fu W-F (2014) Highly efficient photocatalytic hydrogen evolution by nickel phosphide nanoparticles from aqueous solution. Chem Commun 50(72):10427–10429

Cao S, Chen Y, Hou C-C, Lv X-J, Fu W-F (2015a) Cobalt phosphide as a highly active non-precious metal cocatalyst for photocatalytic hydrogen production under visible light irradiation. J Mater Chem A 3(11):6096–6101

Cao S, Chen Y, Kang L, Lin Z, Fu W-F (2015b) Enhanced photocatalytic H2-evolution by immobilizing CdS nanocrystals on ultrathin $Co_{0.85}Se$/RGO–PEI nanosheets. J Mater Chem A 3(36):18711–18717

Cao S, Chen Y, Wang C-J, Lv X-J, Fu W-F (2015c) Spectacular photocatalytic hydrogen evolution using metal-phosphide/CdS hybrid catalysts under sunlight irradiation. Chem Commun 51(41):8708–8711

Cao S, Wang C-J, Lv X-J, Chen Y, Fu W-F (2015d) A highly efficient photocatalytic H_2 evolution system using colloidal CdS nanorods and nickel nanoparticles in water under visible light irradiation. Appl Catal B 162:381–391

Cargnello M, Gasparotto A, Gombac V, Montini T, Barreca D, Fornasiero P (2011) Photocatalytic H_2 and added-value by-products—the role of metal oxide systems in their synthesis from oxygenates. Eur J Inorg Chem 20(28):4309–4323

Carrettin S, Concepción P, Corma A, López Nieto JM, Puntes VF (2004) Nanocrystalline CeO_2 increases the activity of Au for CO oxidation by two orders of magnitude. Angew Chem Int Ed 43(19):2538–2540

Cavalcante WD, Leitao RC, Gehring TA, Angenent LT, Santaella ST (2017) Anaerobic fermentation for n-caproic acid production: a review. Process Biochem 54:106–119

Cavaleiro AJ, Pereira MA, Guedes AP, Stams AJM, Alves MM, Sousa DZ (2016) Conversion of Cn-unsaturated into Cn-2-saturated LCFA can occur uncoupled from methanogenesis in anaerobic bioreactors. Environ Sci Technol 50(6):3082–3090

Chang S-E, Saha S, Kurade MB, Salama E-S, Chang SW, Jang M, Jeon B-H (2018) Improvement of acidogenic fermentation using an acclimatized microbiome. Int J Hydrogen Energy 43(49):22126–22134

Chaudhary A (2022) India eyes lower green hydrogen costs to spur clean energy use. Bloomberg, India

Chen X, Sun Y, Xiu Z, Li X, Zhang D (2006) Stoichiometric analysis of biological hydrogen production by fermentative bacteria. Int J Hydrogen Energy 31(4):539–549

Chen X, Shen S, Guo L, Mao SS (2010) Semiconductor-based photocatalytic hydrogen generation. Chem Rev 110(11):6503–6570

Chen W-T, Chan A, Al-Azri ZHN, Dosado AG, Nadeem MA, Sun-Waterhouse D, Idriss H, Waterhouse GIN (2015a) Effect of TiO_2 polymorph and alcohol sacrificial agent on the activity of Au/TiO_2 photocatalysts for H_2 production in alcohol–water mixtures. J Catal 329:499–513

Chen W-T, Chan A, Sun-Waterhouse D, Moriga T, Idriss H, Waterhouse GIN (2015b) Ni/TiO_2: a promising low-cost photocatalytic system for solar H_2 production from ethanol–water mixtures. J Catal 326:43–53

Chheda JN, Huber GW, Dumesic JA (2007) Liquid-phase catalytic processing of biomass-derived oxygenated

hydrocarbons to fuels and chemicals. Angew Chem Int Ed 46(38):7164–7183

Cortright RD, Davda RR, Dumesic JA (2002) Hydrogen from catalytic reforming of biomass-derived hydrocarbons in liquid water. Nature 418(6901):964–967

Cudjoe D, Chen W, Zhu B (2022) Valorization of food waste into hydrogen: energy potential, economic feasibility and environmental impact analysis. Fuel 324:124476

Dahmen N, Lewandowski I, Zibek S, Weidtmann A (2019) Integrated lignocellulosic value chains in a growing bioeconomy: status quo and perspectives. GCB Bioenergy 11(1):107–117

Das SR, Basak N (2021) Molecular biohydrogen production by dark and photo fermentation from wastes containing starch: recent advancement and future perspective. Bioprocess Biosyst Eng 44(1):1–25

Das A, Han Z, Haghighi MG, Eisenberg R (2013) Photogeneration of hydrogen from water using CdSe nanocrystals demonstrating the importance of surface exchange. PNAS 110(42):16716–16723

Daskalaki VM, Kondarides DI (2009) Efficient production of hydrogen by photo-induced reforming of glycerol at ambient conditions. Catal Today 144(1):75–80

Davda RR, Shabaker JW, Huber GW, Cortright RD, Dumesic JA (2005) A review of catalytic issues and process conditions for renewable hydrogen and alkanes by aqueous-phase reforming of oxygenated hydrocarbons over supported metal catalysts. Appl Catal B 56(1):171–186

de Sá LRV, de Oliveira TC, dos Santos TF, Matos A, Cammarota MC, Oliveira EMM, Ferreira-Leitão VS (2011) Hydrogenase activity monitoring in the fermentative hydrogen production using heat pretreated sludge: a useful approach to evaluate bacterial communities performance. Int J Hydrogen Energy 36(13):7543–7549

Demirbaş A (2001) Biomass resource facilities and biomass conversion processing for fuels and chemicals. Energy Convers Manag 42(11):1357–1378

Devi L, Ptasinski KJ, Janssen FJJG (2003) A review of the primary measures for tar elimination in biomass gasification processes. Biomass Bioenergy 24(2):125–140

Ding H-B, Tan G-YA, Wang J-Y (2010) Caproate formation in mixed-culture fermentative hydrogen production. Bioresour Technol 101(24):9550–9559

DOE (2022) DOE Launches Bipartisan Infrastructure Law's $8 Billion Program for Clean Hydrogen Hubs Across U.S. The U.S. Department of Energy (DOE), Washington, D.C., USA

Drioli E, Giorno L (2009) Membrane operations: innovative separations and transformations. Wiley, Hoboken

Duman G, Akarsu K, Yilmazer A, Keskin Gundogdu T, Azbar N, Yanik J (2018) Sustainable hydrogen production options from food wastes. Int J Hydrogen Energy 43(23):10595–10604

Elreedy A, Fujii M, Tawfik A (2019) Psychrophilic hydrogen production from petrochemical wastewater via anaerobic sequencing batch reactor: techno-economic assessment and kinetic modelling. Int J Hydrogen Energy 44(11):5189–5202

Elsamadony M, Mostafa A, Fujii M, Tawfik A, Pant D (2021) Advances towards understanding long chain fatty acids-induced inhibition and overcoming strategies for efficient anaerobic digestion process. Water Res 190:116732

Eqi M, Shi C, Xie J, Kang F, Qi H, Tan X, Huang Z, Liu J, Guo J (2022) Synergetic effect of Ni–Au bimetal nanoparticles on urchin-like TiO_2 for hydrogen and arabinose co-production by glucose photoreforming. Adv Compos Hybrid Mater 6(1):5

Etemadi H, Soltani T, Yoshida H, Zhang Y, Telfer SG, Buchanan JK, Plieger PG (2022) Synergistic effect of redox dual PdO_x/MnO_x cocatalysts on the enhanced H_2 production potential of a $SnS/\alpha\text{-}Fe_2O_3$ heterojunction via ethanol photoreforming. ACS Omega 7(46):42347–42358

Fang W, Shangguan W (2019) A review on bismuth-based composite oxides for photocatalytic hydrogen generation. Int J Hydrogen Energy 44(2):895–912

Ferraren-De Cagalitan DDT, Abundo MLS (2021) A review of biohydrogen production technology for application towards hydrogen fuel cells. Renew Sustain Energy Rev 151:111413

Fu Q, Saltsburg H, Flytzani-Stephanopoulos M (2003) Active nonmetallic Au and Pt species on ceria-based water-gas shift catalysts. Science 301(5635):935–938

Fu Q, Deng W, Saltsburg H, Flytzani-Stephanopoulos M (2005) Activity and stability of low-content gold–cerium oxide catalysts for the water–gas shift reaction. Appl Catal B 56(1):57–68

Fujita S-i, Kawamori H, Honda D, Yoshida H, Arai M (2016) Photocatalytic hydrogen production from aqueous glycerol solution using NiO/TiO_2 catalysts: effects of preparation and reaction conditions. Appl Catal B 181:818–824

Gao Y, Jiang J, Meng Y, Yan F, Aihemaiti A (2018) A review of recent developments in hydrogen production via biogas dry reforming. Energy Convers Manag 171:133–155

Ghasemzadeh K, Sadati Tilebon SM, Basile A (2016) 17—Membrane reactors for hydrogen production from biomass-derived oxygenates. In: Figoli A, Cassano A, Basile A (eds) Membrane technologies for biorefining. Woodhead Publishing, pp 435–464

Gimbert-Suriñach C, Albero J, Stoll T, Fortage J, Collomb M-N, Deronzier A, Palomares E, Llobet A (2014) Efficient and limiting reactions in aqueous light-induced hydrogen evolution systems using molecular catalysts and quantum dots. J Am Chem Soc 136(21):7655–7661

Godvin Sharmila V, Tamilarasan K, Dinesh Kumar M, Gopalakrishnan K, Sunita V, Adish Kumar S, Rajesh Banu J (2022) Trends in dark biohydrogen production strategy and linkages with transition towards low carbon economy: an outlook, cost-effectiveness, bottlenecks and future scope. Int J Hydrogen Energy 47(34):15309–15332

Gökçek ÖB, Baş F, Muratçobanoğlu H, Demirel S (2023) Investigation of the effects of magnetite addition on biohydrogen production from apple pulp waste. Fuel 339:127475

Granone LI, Sieland F, Zheng N, Dillert R, Bahnemann DW (2018) Photocatalytic conversion of biomass into valuable products: a meaningful approach? Green Chem 20(6):1169–1192

Grootscholten TIM, Strik DPBTB, Steinbusch KJJ, Buisman CJN, Hamelers HVM (2014) Two-stage medium chain fatty acid (MCFA) production from municipal solid waste and ethanol. Appl Energy 116:223–229

Gunawan D, Toe CY, Sun K, Scott J, Amal R (2022) Improved carrier dynamics in nickel/urea-functionalized carbon nitride for ethanol photoreforming. Photochem Photobiol Sci 21(12):2115–2126

Guo S-y, Zhao T-j, Jin Z-q, Wan X-m, Wang P-g, Shang J, Han S (2015) Self-assembly synthesis of precious-metal-free 3D ZnO nano/micro spheres with excellent photocatalytic hydrogen production from solar water splitting. J Power Sources 293:17–22

Han B, Hu YH (2015) Highly efficient temperature-induced visible light photocatalytic hydrogen production from water. J Phys Chem C 119(33):18927–18934

Han Z, Qiu F, Eisenberg R, Holland PL, Krauss TD (2012) Robust photogeneration of H_2 in water using semiconductor nanocrystals and a nickel catalyst. Science 338(6112):1321–1324

Han K, Wang M, Zhang S, Wu S, Yang Y, Sun L (2015) Photochemical hydrogen production from water catalyzed by CdTe quantum dots/molecular cobalt catalyst hybrid systems. Chem Commun 51(32):7008–7011

Hendi AH, Osman AM, Khan I, Saleh TA, Kandiel TA, Qahtan TF, Hossain MK (2020) Visible light-driven photoelectrocatalytic water splitting using Z-scheme Ag-decorated MoS_2/RGO/$NiWO_4$ heterostructure. ACS Omega 5(49):31644–31656

Herman AP, Yusup S, Shahbaz M, Patrick DO (2016) Bottom ash characterization and its catalytic potential in biomass gasification. Proc Eng 148:432–436

Hibino T, Kobayashi K, Ito M, Ma Q, Nagao M, Fukui M, Teranishi S (2018) Efficient hydrogen production by direct electrolysis of waste biomass at intermediate temperatures. ACS Sustain Chem Eng 6(7):9360–9368

Ho K-L, Lee D-J, Su A, Chang J-S (2012) Biohydrogen from lignocellulosic feedstock via one-step process. Int J Hydrogen Energy 37(20):15569–15574

Hu S, Shaner MR, Beardslee JA, Lichterman M, Brunschwig BS, Lewis NS (2014) Amorphous TiO_2 coatings stabilize Si, GaAs, and GaP photoanodes for efficient water oxidation. Science 344(6187):1005–1009

Hu J, Liu A, Jin H, Ma D, Yin D, Ling P, Wang S, Lin Z, Wang J (2015) A versatile strategy for Shish–Kebab-like multi-heterostructured chalcogenides and enhanced photocatalytic hydrogen evolution. J Am Chem Soc 137(34):11004–11010

Huber GW, Dumesic JA (2006) An overview of aqueous-phase catalytic processes for production of hydrogen and alkanes in a biorefinery. Catal Today 111(1):119–132

Huber GW, Shabaker JW, Dumesic JA (2003) Raney Ni–Sn catalyst for H_2 production from biomass-derived hydrocarbons. Science 300(5628):2075–2077

Huber GW, Iborra S, Corma A (2006a) Synthesis of transportation fuels from biomass: chemistry, catalysts, and engineering. Chem Rev 106(9):4044–4098

Huber GW, Shabaker JW, Evans ST, Dumesic JA (2006b) Aqueous-phase reforming of ethylene glycol over supported Pt and Pd bimetallic catalysts. Appl Catal B 62(3):226–235

Jamali NS, Md Jahim J, Wan Isahak WNR (2016) Biofilm formation on granular activated carbon in xylose and glucose mixture for thermophilic biohydrogen production. Int J Hydrogen Energy 41(46):21617–21627

Jiang J, Zhou H, Ding J, Zhang F, Fan T, Zhang D (2015a) Competition between oxidation and anti-oxidation to guarantee visible light activity for a TiO_{2-x} photocatalyst from the dissolution of Ti^0. Int J Hydrogen Energy 40(30):9155–9164

Jiang X, Fu X, Zhang L, Meng S, Chen S (2015b) Photocatalytic reforming of glycerol for H_2 evolution on Pt/TiO_2: fundamental understanding the effect of co-catalyst Pt and the Pt deposition route. J Mater Chem A 3(5):2271–2282

Jiao Y (2021) Chapter 2—Waste to biohydrogen: potential and feasibility. In: Zhang Q, He C, Ren J, Goodsite M (eds) Waste to renewable biohydrogen. Academic Press, pp 33–53

Kalamaras CM, Efstathiou AM (2013) Hydrogen production technologies: current state and future developments. In: Poullikkas A, Al-Assaf Y (eds) Conference papers in science. Hindawi Publishing Corporation, p 690627

Karmee SK (2016) Liquid biofuels from food waste: current trends, prospect and limitation. Renew Sustain Energy Rev 53:945–953

Kim WB, Voitl T, Rodriguez-Rivera GJ, Dumesic JA (2004) Powering fuel cells with CO via aqueous polyoxometalates and gold catalysts. Science 305(5688):1280–1283

Kim WB, Rodriguez-Rivera GJ, Evans ST, Voitl T, Einspahr JJ, Voyles PM, Dumesic JA (2005a) Catalytic oxidation of CO by aqueous polyoxometalates on carbon-supported gold nanoparticles. J Catal 235(2):327–332

Kim WB, Voitl T, Rodriguez-Rivera GJ, Evans ST, Dumesic JA (2005b) Preferential oxidation of CO in H_2 by aqueous polyoxometalates over metal catalysts. Angew Chem Int Ed 44(5):778–782

Kim D, Vardon DR, Murali D, Sharma BK, Strathmann TJ (2016) Valorization of waste lipids through hydrothermal catalytic conversion to liquid hydrocarbon fuels with in situ hydrogen production. ACS Sustain Chem Eng 4(3):1775–1784

Kondarides DI, Daskalaki VM, Patsoura A, Verykios XE (2008) Hydrogen production by photo-induced reforming of biomass components and derivatives at ambient conditions. Catal Lett 122:26–32

Koty AC (2022) China's hydrogen energy industry: state policy, investment opportunities. China briefing. Dezan Shira & Associates

Kozlova EA, Markovskaya DV, Cherepanova SV, Saraev AA, Gerasimov EY, Perevalov TV, Kaichev VV, Parmon VN (2014) Novel photocatalysts based on $Cd_{1-x}Zn_xS$/$Zn(OH)_2$ for the hydrogen evolution from water solutions of ethanol. Int J Hydrogen Energy 39(33):18758–18769

Kucek LA, Spirito CM, Angenent LT (2016a) High n-caprylate productivities and specificities from dilute ethanol and acetate: chain elongation with microbiomes to upgrade products from syngas fermentation. Energy Environ Sci 9(11):3482–3494

Kucek LA, Xu J, Nguyen M, Angenent LT (2016b) Waste conversion into n-caprylate and n-caproate: resource

recovery from wine lees using anaerobic reactor microbiomes and in-line extraction. Front Microbiol 7:1892
Kum JM, Park YJ, Kim HJ, Cho SO (2015) Plasmon-enhanced photocatalytic hydrogen production over visible-light responsive Cu/TiO_2. Nanotechnology 26(12):125402
Lane B, Reed J, Shaffer B, Samuelsen S (2021) Forecasting renewable hydrogen production technology shares under cost uncertainty. Int J Hydrogen Energy 46(54):27293–27306
Lang D, Shen T, Xiang Q (2015) Roles of MoS_2 and graphene as cocatalysts in the enhanced visible-light photocatalytic H_2 production activity of multiarmed CdS nanorods. ChemCatChem 7(6):943–951
Latorre-Sánchez M, Primo A, García H (2013) P-doped graphene obtained by pyrolysis of modified alginate as a photocatalyst for hydrogen generation from water-methanol mixtures. Angew Chem Int Ed 52(45):11813–11816
Lee H-S, Salerno MB, Rittmann BE (2008) Thermodynamic evaluation on H_2 production in glucose fermentation. Environ Sci Technol 42(7):2401–2407
Lee D-J, Show K-Y, Su A (2011) Dark fermentation on biohydrogen production: pure culture. Bioresour Technol 102(18):8393–8402
Lewis MA, Serban M, Basco JK (2003) Hydrogen production at < 550 °C using a low temperature thermochemical cycle. Nuclear production of hydrogen second information exchange meeting. Organisation for Economic Cooperation and Development (OECD), Argonne, Illinois, USA, pp 145–156
Li C, Xi Z, Fang W, Xing M, Zhang J (2015a) Enhanced photocatalytic hydrogen evolution activity of $CuInS_2$ loaded TiO_2 under solar light irradiation. J Solid State Chem 226:94–100
Li J, Pan X, Xu Y, Jia L, Yi X, Fang W (2015b) Synergetic effect of copper species as cocatalyst on $LaFeO_3$ for enhanced visible-light photocatalytic hydrogen evolution. Int J Hydrogen Energy 40(40):13918–13925
Li W, Cheng C, He L, Liu M, Cao G, Yang S, Ren N (2021) Effects of feedstock and pyrolysis temperature of biochar on promoting hydrogen production of ethanol-type fermentation. Sci Total Environ 790:148206
Liguras DK, Goundani K, Verykios XE (2004) Production of hydrogen for fuel cells by catalytic partial oxidation of ethanol over structured Ru catalysts. Int J Hydrogen Energy 29(4):419–427
Liu K, Song C, Subramani V (2009) Hydrogen and syngas production and purification technologies. Wiley, Hoboken
Liu H, Zhao K, Wang T, Deng J, Zeng H (2015a) Facile preparation of cerium (Ce) and antimony (Sb) codoped SnO_2 for hydrogen production in lactic acid solution. Mater Sci Semicond Process 40:670–675
Liu J, Liu Y, Liu N, Han Y, Zhang X, Huang H, Lifshitz Y, Lee S-T, Zhong J, Kang Z (2015b) Metal-free efficient photocatalyst for stable visible water splitting via a two-electron pathway. Science 347(6225):970–974
Lopes PAL, Mascarenhas AJS, Silva LA (2015) Sonochemical synthesis of $Cd_{1-x}Zn_xS$ solid solutions for application in photocatalytic reforming of glycerol to produce hydrogen. J Alloys Compd 649:332–336
López CR, Melián EP, Ortega Méndez JA, Santiago DE, Doña Rodríguez JM, González Díaz O (2015) Comparative study of alcohols as sacrificial agents in H_2 production by heterogeneous photocatalysis using Pt/TiO_2 catalysts. J Photochem Photobiol A 312:45–54
Lu GQ, Diniz da Costa JC, Duke M, Giessler S, Socolow R, Williams RH, Kreutz T (2007) Inorganic membranes for hydrogen production and purification: a critical review and perspective. J Colloid Interface Sci 314(2):589–603
Lu L, Williams NB, Turner JA, Maness P-C, Gu J, Ren ZJ (2017) Microbial photoelectrosynthesis for self-sustaining hydrogen generation. Environ Sci Technol 51(22):13494–13501
Lv R, Wang X, Lv W, Xu Y, Ge Y, He H, Li G, Wu X, Li X, Li Q (2015) Facile synthesis of ZnO nanorods grown on graphene sheets and its enhanced photocatalytic efficiency. J Chem Technol Biotechnol 90(3):550–558
Mahmod SS, Jahim JM, Abdul PM, Luthfi AAI, Takriff MS (2021) Techno-economic analysis of two-stage anaerobic system for biohydrogen and biomethane production from palm oil mill effluent. J Environ Chem Eng 9(4):105679
Mahoney L, Peng R, Wu C-M, Baltrusaitis J, Koodali RT (2015) Solar simulated hydrogen evolution using cobalt oxide nanoclusters deposited on titanium dioxide mesoporous materials prepared by evaporation induced self-assembly process. Int J Hydrogen Energy 40(34):10795–10806
Malato S, Maldonado MI, Fernández-Ibáñez P, Oller I, Polo I, Sánchez-Moreno R (2016) Decontamination and disinfection of water by solar photocatalysis: the pilot plants of the plataforma solar de Almeria. Mater Sci Semicond Process 42:15–23
Martha S, Chandra Sahoo P, Parida KM (2015) An overview on visible light responsive metal oxide based photocatalysts for hydrogen energy production. RSC Adv 5(76):61535–61553
Megía PJ, Vizcaíno AJ, Calles JA, Carrero A (2021) Hydrogen production technologies: from fossil fuels toward renewable sources. A mini review. Energy Fuels 35(20):16403–16415
Miyazawa T, Kimura T, Nishikawa J, Kado S, Kunimori K, Tomishige K (2006) Catalytic performance of supported Ni catalysts in partial oxidation and steam reforming of tar derived from the pyrolysis of wood biomass. Catal Today 115(1):254–262
Mohd Jamaludin NF, Jamali NS, Abdullah LC, Idrus S, Engliman NS, Abdul PM (2023) Biohydrogen production with utilisation of magnetite nanoparticles embedded in granular activated carbon from coconut shell. Int J Hydrogen Energy. https://doi.org/10.1016/j.ijhydene.2022.12.073
Moretti G, Fierro G, Ferraris G, Andreozzi GB, Naticchioni V (2014) N_2O decomposition over [Fe]-MFI catalysts: Influence of the FexOy nuclearity and the presence of framework aluminum on the catalytic activity. J Catal 318:1–13
Moya A, Cherevan A, Marchesan S, Gebhardt P, Prato M, Eder D, Vilatela JJ (2015) Oxygen vacancies and interfaces enhancing photocatalytic hydrogen production in mesoporous CNT/TiO_2 hybrids. Appl Catal B 179:574–582
Munusamy TD, Chin SY, Rahman Khan MM (2022) Photoreforming hydrogen production by carbon doped exfoliated

g-C_3N_4: optimization using design expert®software. Mater Today Proc 57:1162–1168

Musso M, Veiga S, De León A, Quevedo A, Bussi J (2023) Characterization and application of a bismuth titanate $Bi_2Ti_2O_7$ synthetized through a solvothermal route for glycerol photooxidation and photoreforming. Mater Lett 330:133346

Nagaraju G, Manjunath K, Sarkar S, Gunter E, Teixeira SR, Dupont J (2015) TiO_2–RGO hybrid nanomaterials for enhanced water splitting reaction. Int J Hydrogen Energy 40(36):12209–12216

Naikoo GA, Arshad F, Hassan IU, Tabook MA, Pedram MZ, Mustaqeem M, Tabassum H, Ahmed W, Rezakazemi M (2021) Thermocatalytic hydrogen production through decomposition of methane—a review. Front Chem 9:736801

Nakano J (2021) Japan's hydrogen industrial strategy. The Center for Strategic and International Studies (CSIS), NW Washington, DC, USA

Nakano J (2022) China's hydrogen industrial strategy. The Center for Strategic and International Studies (CSIS), NW Washington, DC, USA

Naldoni A, Altomare M, Zoppellaro G, Liu N, Kment Š, Zbořil R, Schmuki P (2019) Photocatalysis with reduced TiO_2: from black TiO_2 to cocatalyst-free hydrogen production. ACS Catal 9(1):345–364

Nalley S, LaRose A (2021) International energy outlook 2021. U.S. Energy Information Administration, Washington, DC, USA

Nasr N, Elbeshbishy E, Hafez H, Nakhla G, El Naggar MH (2011) Bio-hydrogen production from thin stillage using conventional and acclimatized anaerobic digester sludge. Int J Hydrogen Energy 36(20):12761–12769

Nasr N, Velayutham P, Elbeshbishy E, Nakhla G, El Naggar MH, Khafipour E, Derakhshani H, Levin DB, Hafez H (2015) Effect of headspace carbon dioxide sequestration on microbial biohydrogen communities. Int J Hydrogen Energy 40(32):9966–9976

Navarro RM, Peña MA, Fierro JLG (2007) Hydrogen production reactions from carbon feedstocks: fossil fuels and biomass. Chem Rev 107(10):3952–3991

Navarro RM, Sánchez-Sánchez MC, Alvarez-Galvan MC, Valle Fd, Fierro JLG (2009) Hydrogen production from renewable sources: biomass and photocatalytic opportunities. Energy Environ Sci 2(1):35–54

Nurul-Adela B, Nasrin A-B, Loh S-K (2016) Palm oil mill effluent as a low-cost substrate for bioflocculant production by *Bacillus marisflavi* NA8. Bioresour Bioprocess 3(1):20

Orozco RS, Hernandez PB, Morales GR, Nunez FU, Villafuerte JO, Lugo VL, Ramirez NF, Diaz CEB, Vazquez PC (2014) Characterization of lignocellulosic fruit waste as an alternative feedstock for bioethanol production. BioResources 9(2):1873–1885

Ozmihci S (2017) Performance of batch solid state fermentation for hydrogen production using ground wheat residue. Int J Hydrogen Energy 42(37):23494–23499

Pachiega R, Rodrigues MF, Rodrigues CV, Sakamoto IK, Varesche MBA, De Oliveira JE, Maintinguer SI (2019) Hydrogen bioproduction with anaerobic bacteria consortium from brewery wastewater. Int J Hydrogen Energy 44(1):155–163

Panmand RP, Sethi YA, Kadam SR, Tamboli MS, Nikam LK, Ambekar JD, Park C-J, Kale BB (2015) Self-assembled hierarchical nanostructures of $Bi2WO_6$ for hydrogen production and dye degradation under solar light. CrystEngComm 17(1):107–115

Parthasarathy P, Narayanan KS (2014) Hydrogen production from steam gasification of biomass: influence of process parameters on hydrogen yield—a review. Renew Energ 66:570–579

Peng J, Zhou Y, Wang H, Zhou H, Cai S (2015a) Hydrothermal synthesis and formation mechanism of photocatalytically active $SrTiO_3$ nanocrystals using anatase TiO_2 with different facets as a precursor. CrystEngComm 17(8):1805–1812

Peng Y, Shang L, Cao Y, Wang Q, Zhao Y, Zhou C, Bian T, Wu L-Z, Tung C-H, Zhang T (2015b) Effects of surfactants on visible-light-driven photocatalytic hydrogen evolution activities of $AgInZn_7S_9$ nanorods. Appl Surf Sci 358:485–490

Peng S, Ding M, Yi T, Zhan Z, Li Y (2016) Photocatalytic hydrogen evolution and decomposition of glycerol over $Cd_{0.5}Zn_{0.5}S$ solid solution under visible light irradiation. Environ Prog Sustain Energy 35(1):141–148

Petala A, Ioannidou E, Georgaka A, Bourikas K, Kondarides DI (2015) Hysteresis phenomena and rate fluctuations under conditions of glycerol photo-reforming reaction over CuO_x/TiO_2 catalysts. Appl Catal B 178:201–209

Pi Y, Feng X, Song Y, Xu Z, Li Z, Lin W (2020) Metal-organic frameworks integrate Cu photosensitizers and secondary building unit-supported Fe catalysts for photocatalytic hydrogen evolution. J Am Chem Soc 142(23):10302–10307

Prabakar D, Manimudi VT, Suvetha KS, Sampath S, Mahapatra DM, Rajendran K, Pugazhendhi A (2018) Advanced biohydrogen production using pretreated industrial waste: outlook and prospects. Renew Sustain Energy Rev 96:306–324

Praveen Kumar D, Lakshmana Reddy N, Mamatha Kumari M, Srinivas B, Durga Kumari V, Sreedhar B, Roddatis V, Bondarchuk O, Karthik M, Neppolian B, Shankar MV (2015) Cu_2O-sensitized TiO_2 nanorods with nanocavities for highly efficient photocatalytic hydrogen production under solar irradiation. Sol Energy Mater Sol Cells 136:157–166

Puga AV (2016) Photocatalytic production of hydrogen from biomass-derived feedstocks. Coord Chem Rev 315:1–66

Qyyum MA, Ismail S, Ni S-Q, Ihsanullah I, Ahmad R, Khan A, Tawfik A, Nizami A-S, Lee M (2022) Harvesting biohydrogen from industrial wastewater: production potential, pilot-scale bioreactors, commercialization status, techno-economics, and policy analysis. J Clean Prod 340:130809

Reaume S (2009) Fermentation of glucose and xylose to hydrogen in the presenceof long chain fatty acids. Faculty of Graduate Studies, University of Windsor, Windsor, p 128

Ren Y, Si B, Liu Z, Jiang W, Zhang Y (2022) Promoting dark fermentation for biohydrogen production: potential roles of iron-based additives. Int J Hydrogen Energy 47(3):1499–1515

Rioche C, Kulkarni S, Meunier FC, Breen JP, Burch R (2005) Steam reforming of model compounds and fast pyrolysis bio-oil on supported noble metal catalysts. Appl Catal B 61(1):130–139

Romero Ocaña I, Beltram A, Delgado Jaén JJ, Adami G, Montini T, Fornasiero P (2015) Photocatalytic H_2 production by ethanol photodehydrogenation: effect of anatase/brookite nanocomposites composition. Inorg Chim Acta 431:197–205

Rostrup-Nielsen JR (2001) Conversion of hydrocarbons and alcohols for fuel cells. Phys Chem Chem Phys 3(3):283–288

Rueda-Navarro CM, Ferrer B, Baldoví HG, Navalón S (2022) Photocatalytic hydrogen production from glycerol aqueous solutions as sustainable feedstocks using Zr-based UiO-66 materials under simulated sunlight irradiation. Nanomater 12(21):3808

Saha S, Kurade MB, El-Dalatony MM, Chatterjee PK, Lee DS, Jeon B-H (2016) Improving bioavailability of fruit wastes using organic acid: an exploratory study of biomass pretreatment for fermentation. Energy Convers Manag 127:256–264

Saha S, Jeon B-H, Kurade MB, Jadhav SB, Chatterjee PK, Chang SW, Govindwar SP, Kim SJ (2018) Optimization of dilute acetic acid pretreatment of mixed fruit waste for increased methane production. J Clean Prod 190:411–421

Saha S, Jeon B-H, Kurade MB, Chatterjee PK, Chang SW, Markkandan K, Salama E-S, Govindwar SP, Roh H-S (2019) Microbial acclimatization to lipidic-waste facilitates the efficacy of acidogenic fermentation. Chem Eng J 358:188–196

Saha S, Basak B, Hwang J-H, Salama E-S, Chatterjee PK, Jeon B-H (2020) Microbial symbiosis: a network towards biomethanation. Trends Microbiol 28(12):968–984

Saidi R, Liebgott PP, Gannoun H, Ben Gaida L, Miladi B, Hamdi M, Bouallagui H, Auria R (2018) Biohydrogen production from hyperthermophilic anaerobic digestion of fruit and vegetable wastes in seawater: simplification of the culture medium of *Thermotoga maritima*. Waste Manage (oxford) 71:474–484

Salama E-S, Saha S, Kurade MB, Dev S, Chang SW, Jeon B-H (2019) Recent trends in anaerobic co-digestion: fat, oil, and grease (FOG) for enhanced biomethanation. Prog Energy Combust Sci 70:22–42

Santhanam KSV, Press RJ, Miri MJ, Bailey AV, Takacs GA (2017) Introduction to hydrogen technology, 2nd edn. Wiley

Sarangi PK, Nanda S (2020) Biohydrogen production through dark fermentation. Chem Eng Technol 43(4):601–612

Schneider J, Matsuoka M, Takeuchi M, Zhang J, Horiuchi Y, Anpo M, Bahnemann DW (2014) Understanding TiO_2 photocatalysis: mechanisms and materials. Chem Rev 114(19):9919–9986

Serra M, Albero J, García H (2015) Photocatalytic activity of Au/TiO_2 photocatalysts for H_2 evolution: role of the Au nanoparticles as a function of the irradiation wavelength. ChemPhysChem 16(9):1842–1845

Shabaker JW, Huber GW, Dumesic JA (2004) Aqueous-phase reforming of oxygenated hydrocarbons over Sn-modified Ni catalysts. J Catal 222(1):180–191

Sharma P, Melkania U (2017) Biochar-enhanced hydrogen production from organic fraction of municipal solid waste using co-culture of *Enterobacter aerogenes* and *E. coli*. Int J Hydrogen Energy 42(30):18865–18874

Shen L, Luo M, Liu Y, Liang R, Jing F, Wu L (2015) Noble-metal-free MoS_2 co-catalyst decorated UiO-66/CdS hybrids for efficient photocatalytic H_2 production. Appl Catal B 166–167:445–453

Sikarwar VS, Zhao M, Clough P, Yao J, Zhong X, Memon MZ, Shah N, Anthony EJ, Fennell PS (2016) An overview of advances in biomass gasification. Energy Environ Sci 9(10):2939–2977

Silva CG, Sampaio MJ, Marques RRN, Ferreira LA, Tavares PB, Silva AMT, Faria JL (2015) Photocatalytic production of hydrogen from methanol and saccharides using carbon nanotube-TiO_2 catalysts. Appl Catal B 178:82–90

Singh S, Jain S, Ps V, Tiwari AK, Nouni MR, Pandey JK, Goel S (2015) Hydrogen: a sustainable fuel for future of the transport sector. Renew Sustain Energy Rev 51:623–633

Sołowski G, Shalaby MS, Abdallah H, Shaban AM, Cenian A (2018) Production of hydrogen from biomass and its separation using membrane technology. Renew Sustain Energy Rev 82:3152–3167

Sołowski G, Konkol I, Cenian A (2020) Production of hydrogen and methane from lignocellulose waste by fermentation. A review of chemical pretreatment for enhancing the efficiency of the digestion process. J Clean Prod 267:121721

Song T, Zhang P, Zeng J, Wang T, Ali A, Zeng H (2017) Tunable conduction band energy and metal-to-ligand charge transfer for wide-spectrum photocatalytic H_2 evolution and stability from isostructural metal-organic frameworks. Int J Hydrogen Energy 42(43):26605–26616

Speltini A, Sturini M, Maraschi F, Dondi D, Fisogni G, Annovazzi E, Profumo A, Buttafava A (2015) Evaluation of UV-A and solar light photocatalytic hydrogen gas evolution from olive mill wastewater. Int J Hydrogen Energy 40(12):4303–4310

Spirito CM, Richter H, Rabaey K, Stams AJM, Angenent LT (2014) Chain elongation in anaerobic reactor microbiomes to recover resources from waste. Curr Opin Biotechnol 27(C):115–122

Stegbauer L, Schwinghammer K, Lotsch BV (2014) A hydrazone-based covalent organic framework for photocatalytic hydrogen production. Chem Sci 5(7):2789–2793

Stichnothe H, Azapagic A (2009) Bioethanol from waste: life cycle estimation of the greenhouse gas saving potential. Resour Conserv Recycl 53(11):624–630

Sun T, Liu E, Liang X, Hu X, Fan J (2015) Enhanced hydrogen evolution from water splitting using Fe–Ni codoped and Ag deposited anatase TiO_2 synthesized by solvothermal method. Appl Surf Sci 347:696–705

Sun Y, Yang G, Zhang J, Wen C, Sun Z (2019a) Optimization and kinetic modeling of an enhanced bio-hydrogen fermentation with the addition of synergistic biochar and nickel nanoparticle. Int J Energy Res 43(2):983–999

Sun Z, Zhu M, Lv X, Liu Y, Shi C, Dai Y, Wang A, Majima T (2019b) Insight into iron group transition metal phosphides (Fe_2P, Co_2P, Ni_2P) for improving photocatalytic hydrogen generation. Appl Catal B 246:330–336

Sutton D, Kelleher B, Ross JRH (2001) Review of literature on catalysts for biomass gasification. Fuel Process Technol 73(3):155–173

Taherdanak M, Zilouei H, Karimi K (2015) Investigating the effects of iron and nickel nanoparticles on dark hydrogen fermentation from starch using central composite design. Int J Hydrogen Energy 40(38):12956–12963

Taipabu MI, Viswanathan K, Wu W, Hattu N, Atabani AE (2022) A critical review of the hydrogen production from biomass-based feedstocks: challenge, solution, and future prospect. Process Saf Environ Prot 164:384–407

Talavera-Caro AG, Sánchez-Muñoz MA, Lira IOH-D, Montañez-Hernández LE, Hernández-Almanza AY, Morlett-Chávez JA, MdlM E-P, Balagurusamy N (2020) Proteomics of lignocellulosic substrates bioconversion in anaerobic digesters to increase carbon recovery as methane. In: Zakaria ZA, Boopathy R, Dib JR (eds) Valorisation of agro-industrial residues—biological approaches, vol I. Springer, Cham, pp 81–110

Tanaka A, Hashimoto K, Kominami H (2014) Visible-light-induced hydrogen and oxygen formation over $Pt/Au/WO_3$ photocatalyst utilizing two types of photoabsorption due to surface plasmon resonance and band-gap excitation. J Am Chem Soc 136(2):586–589

Tawfik A, Ali M, Danial A, Zhao S, Meng F, Nasr M (2021a) 2-biofuels (H_2 and CH_4) production from anaerobic digestion of biscuits wastewater: experimental study and techno-economic analysis. J Water Process Eng 39:101736

Tawfik A, Nasr M, Galal A, El-Qelish M, Yu Z, Hassan MA, Salah HA, Hasanin MS, Meng F, Bokhari A, Qyyum MA, Lee M (2021b) Fermentation-based nanoparticle systems for sustainable conversion of black-liquor into biohydrogen. J Clean Prod 309:127349

Tekade SP, Pednekar AS, Jadhav GR, Kalekar SE, Shende DZ, Wasewar KL (2020) Hydrogen generation through water splitting reaction using waste aluminum in presence of gallium. Int J Hydrogen Energy 45(44):23954–23965

Tomishige K, Asadullah M, Kunimori K (2004) Syngas production by biomass gasification using $Rh/CeO_2/SiO_2$ catalysts and fluidized bed reactor. Catal Today 89(4):389–403

Tu H, Xu L, Mou F, Guan J (2015) Single crystalline tantalum oxychloride microcubes: controllable synthesis, formation mechanism and enhanced photocatalytic hydrogen production activity. Chem Commun 51(62):12455–12458

Tu W, Xu Y, Wang J, Zhang B, Zhou T, Yin S, Wu S, Li C, Huang Y, Zhou Y, Zou Z, Robertson J, Kraft M, Xu R (2017) Investigating the role of tunable nitrogen vacancies in graphitic carbon nitride nanosheets for efficient visible-light-driven H_2 evolution AND CO_2 reduction. ACS Sustain Chem Eng 5(8):7260–7268

Usino DO, Ylitervo P, Moreno A, Sipponen MH, Richards T (2021) Primary interactions of biomass components during fast pyrolysis. J Anal Appl Pyrolysis 159:105297

Vaidya PD, Lopez-Sanchez JA (2017) Review of hydrogen production by catalytic aqueous-phase reforming. ChemistrySelect 2(22):6563–6576

Venkata Mohan S, Agarwal L, Mohanakrishna G, Srikanth S, Kapley A, Purohit HJ, Sarma PN (2011) Firmicutes with iron dependent hydrogenase drive hydrogen production in anaerobic bioreactor using distillery wastewater. Int J Hydrogen Energy 36(14):8234–8242

Vispute TP, Huber GW (2009) Production of hydrogen, alkanes and polyols by aqueous phase processing of wood-derived pyrolysis oils. Green Chem 11(9):1433–1445

Wan J, Jing Y, Zhang S, Angelidaki I, Luo G (2016) Mesophilic and thermophilic alkaline fermentation of waste activated sludge for hydrogen production: focusing on homoacetogenesis. Water Res 102:524–532

Wang J, Yin Y (2021) *Clostridium* species for fermentative hydrogen production: an overview. Int J Hydrogen Energy 46(70):34599–34625

Wang X, Peng W-c, Li X-y (2014) Photocatalytic hydrogen generation with simultaneous organic degradation by composite CdS–ZnS nanoparticles under visible light. Int J Hydrogen Energy 39(25):13454–13461

Wang C, Zhang X, Wei Y, Kong L, Chang F, Zheng H, Wu L, Zhi J, Liu Y (2015a) Correlation between band alignment and enhanced photocatalysis: a case study with anatase/TiO_2(B) nanotube heterojunction. Dalton Trans 44(29):13331–13339

Wang P, Zhang J, He H, Xu X, Jin Y (2015b) The important role of surface ligand on CdSe/CdS core/shell nanocrystals in affecting the efficiency of H_2 photogeneration from water. Nanoscale 7(13):5767–5775

Wang X, Yu H, Yang L, Shao L, Xu L (2015c) A highly efficient and noble metal-free photocatalytic system using Ni_xB/CdS as photocatalyst for visible light H_2 production from aqueous solution. Catal Commun 67:45–48

Weimer PJ, Nerdahl M, Brandl DJ (2015) Production of medium-chain volatile fatty acids by mixed ruminal microorganisms is enhanced by ethanol in co-culture with *Clostridium kluyveri*. Bioresour Technol 175:97–101

Wu L, Moteki T, Gokhale Amit A, Flaherty David W, Toste FD (2016) Production of fuels and chemicals from biomass: condensation reactions and beyond. Chem 1(1):32–58

Wulf C, Kaltschmitt M (2012) Life cycle assessment of hydrogen supply chain with special attention on hydrogen refuelling stations. Int J Hydrogen Energy 37(21):16711–16721

Xiang Q, Cheng B, Yu J (2015) Graphene-based photocatalysts for solar-fuel generation. Angew Chem Int Ed 54(39):11350–11366

Xitao W, Rong L, Kang W (2014) Synthesis of ZnO@ZnS–Bi_2S_3 core–shell nanorod grown on reduced graphene oxide sheets and its enhanced photocatalytic performance. J Mater Chem A 2(22):8304–8313

Xu Y, Xu R (2015) Nickel-based cocatalysts for photocatalytic hydrogen production. Appl Surf Sci 351:779–793

Xu Z, Xu S, Li N, Wu F, Chen S, Lu W, Chen W (2017) Waste-to-energy conversion on graphitic carbon nitride: utilizing the transformation of macrolide antibiotics to enhance photoinduced hydrogen production. ACS Sustain Chem Eng 5(11):9667–9672

Xue Y, Wang X (2015) The effects of Ag doping on crystalline structure and photocatalytic properties of $BiVO_4$. In J Hydrogen Energy 40(17):5878–5888

Yang G, Wang J (2017) Co-fermentation of sewage sludge with ryegrass for enhancing hydrogen production:

performance evaluation and kinetic analysis. Bioresour Technol 243:1027–1036

Yang G, Wang J (2018a) Enhancement of biohydrogen production from grass by ferrous ion and variation of microbial community. Fuel 233:404–411

Yang G, Wang J (2018b) Improving mechanisms of biohydrogen production from grass using zero-valent iron nanoparticles. Bioresour Technol 266:413–420

Yang G, Wang J (2019) Synergistic enhancement of biohydrogen production from grass fermentation using biochar combined with zero-valent iron nanoparticles. Fuel 251:420–427

Yang X, Wu L, Du L, Li X (2015) Photocatalytic water splitting towards hydrogen production on gold nanoparticles (NPs) entrapped in TiO_2 nanotubes. Catal Lett 145(9):1771–1777

Ye S, Wang R, Wu M-Z, Yuan Y-P (2015) A review on g-C_3N_4 for photocatalytic water splitting and CO_2 reduction. Appl Surf Sci 358:15–27

Yilmaz C, Koyuncu I, Alcin M, Tuna M (2019) Artificial neural networks based thermodynamic and economic analysis of a hydrogen production system assisted by geothermal energy on field programmable gate array. Int J Hydrogen Energy 44(33):17443–17459

Yin Y, Wang J (2019) Enhanced biohydrogen production from macroalgae by zero-valent iron nanoparticles: Insights into microbial and metabolites distribution. Bioresour Technol 282:110–117

Yue Q, Wan Y, Sun Z, Wu X, Yuan Y, Du P (2015) MoP is a novel, noble-metal-free cocatalyst for enhanced photocatalytic hydrogen production from water under visible light. J Mater Chem A 3(33):16941–16947

Yukesh Kannah R, Kavitha S, Preethi P, Karthikeyan O, Kumar G, Dai-Viet NV, Rajesh Banu J (2021) Techno-economic assessment of various hydrogen production methods—a review. Bioresour Technol 319:124175

Yuksel YE, Ozturk M (2017) Thermodynamic and thermo-economic analyses of a geothermal energy based integrated system for hydrogen production. Int J Hydrogen Energy 42(4):2530–2546

Yun Y-M, Shin H-S, Kim D-H (2016) Feasibility study of SCFAs production from microalgae during hydrogen fermentation. Int J Hydrogen Energy 41(7):4439–4445

Zhang L, Zhang L, Li D (2015a) Enhanced dark fermentative hydrogen production by zero-valent iron activated carbon micro-electrolysis. Int J Hydrogen Energy 40(36):12201–12208

Zhang X, Peng B, Zhang S, Peng T (2015b) Robust wide visible-light-responsive photoactivity for H_2 production over a polymer/polymer heterojunction photocatalyst: the significance of sacrificial reagent. ACS Sustain Chem Eng 3(7):1501–1509

Zhao Y, Lu Y, Chen L, Wei X, Zhu J, Zheng Y (2020) Redox dual-cocatalyst-modified CdS double-heterojunction photocatalysts for efficient hydrogen production. ACS Appl Mater Interfaces 12(41):46073–46083

Zhong W, Wang C, Jiang B, Peng S, Zhao H, Shu R, Tian Z, Du Y, Chen Y (2022) Investigation on multifunctional Au/TiO_2@n-octadecane microcapsules towards catalytic photoreforming hydrogen production and photothermal conversion. Int J Hydrogen Energy 47(98):41540–41552

Zhou J-J, Wang R, Liu X-L, Peng F-M, Li C-H, Teng F, Yuan Y-P (2015) In situ growth of CdS nanoparticles on UiO-66 metal–organic framework octahedrons for enhanced photocatalytic hydrogen production under visible light irradiation. Appl Surf Sci 346:278–283

Zhou M, Yan B, Wong JWC, Zhang Y (2018) Enhanced volatile fatty acids production from anaerobic fermentation of food waste: a mini-review focusing on acidogenic metabolic pathways. Bioresour Technol 248:68–78

Zhu Y, Lin Q, Zhong Y, Tahini HA, Shao Z, Wang H (2020) Metal oxide-based materials as an emerging family of hydrogen evolution electrocatalysts. Energy Environ Sci 13(10):3361–3392

Zinoviev S, Müller-Langer F, Das P, Bertero N, Fornasiero P, Kaltschmitt M, Centi G, Miertus S (2010) Next-generation biofuels: survey of emerging technologies and sustainability issues. Chemsuschem 3(10):1106–1133